

A model-based infrastructure for the specification and runtime execution of self-adaptive IoT architectures

Iván Alfonso^{1,2*}, Kelly Garcés¹, Harold Castro¹ and Jordi Cabot^{2,3}

^{1*}Department of Systems and Computing Engineering,
Universidad de los Andes, Bogotá, Colombia.

²Universitat Obertat de Catalunya, Barcelona, Spain.

³ICREA, Barcelona, Spain.

*Corresponding author(s). E-mail(s): id.alfonso@uniandes.edu.co;
Contributing authors: kj.garces971@uniandes.edu.co;
hcastro@uniandes.edu.co; jordi.cabot@icrea.cat;

Abstract

To meet increasingly restrictive requirements and improve quality of service (QoS), Internet of Things (IoT) systems have embraced multi-layered architectures leveraging edge and fog computing. However, the dynamic and changing IoT environment can impact QoS due to unexpected events. Therefore, proactive evolution and adaptation of the IoT system becomes a necessity and concern. In this paper, we present a model-based approach for the specification and execution of self-adaptive multi-layered IoT systems. Our proposal comprises the design of a domain-specific language (DSL) for the specification of such architectures, and a runtime framework to support the system behavior and its self-adaptation at runtime. The code for the deployment of the IoT system and the execution of the runtime framework is automatically produced by our prototype code generator. Moreover, we also show and validate the extensibility of such DSL by applying it to the domain of underground mining. The complete infrastructure (modeling tool, generator and runtime components) is available in an online open source repository.

Keywords: Domain-specific language, Internet of Things, Self-adaptive system, Edge computing, Fog computing

1 Introduction

Nowadays, billions of connected devices sense, communicate, and share information about their environment. To manage all these devices, traditional Internet of Things (IoT) systems rely on cloud-based architectures, which allocate all processing and storage capabilities to cloud servers. Although cloud-based IoT architectures have advantages such as reduced maintenance costs and application development efforts, they also have limitations in bandwidth and communication delays [1]. Given these limitations, edge and fog computing have emerged with the goal of distributing processing and storage closer to data sources (i.e. things). As a result, new IoT systems aim to leverage the advantages of edge, fog, and cloud computing by following a multi-layered architecture.

Nevertheless, creating such complex designs is a challenging task. Even more challenging is managing and adapting IoT systems at runtime to ensure the optimal performance of the system while facing changes in the environmental conditions. Indeed, IoT systems are commonly exposed to changing environments that induce unexpected events at runtime (such as unstable signal strength, latency growth, and software failures) that can impact its Quality of Service (QoS). To deal with such events, a number of runtime adaptation rules should be automatically applied, e.g. *architectural adaptations* such as auto-scaling and offloading tasks.

In this sense, a better support to define and execute complex IoT systems and their (self)adaptation rules to semi-automate the deployment and evolution process is necessary [2]. A usual strategy when it comes to modeling complex domains is to develop a domain-specific language (DSL) for that domain [3]. In short, a DSL offers a set of abstractions and vocabulary closer to the one already employed by domain experts. Nevertheless, current IoT modeling approaches do not typically cover multi-layered architectures [4–7] and even less include a sublanguage to ease the definition of the dynamic rules governing the IoT system. Our research aims at overcoming this situation by presenting a model-based infrastructure for the specification and runtime execution of multi-layered IoT architectures, including self-adaptation rules. Our proposal combines a DSL for the specification of static and dynamic aspects of this type of systems together with a runtime infrastructure and a code-generator able to semi-automate their deployment and runtime monitoring and adaptation.

This work is an extension of our study presented in [8], in which we proposed a first version of a DSL for IoT systems and a proof of concept of a code generator. The current work extends this previous contribution to the following aspects:

- Metamodel improvement: we have enhanced the metamodel to support modeling new DSL concepts such as sensor threshold values, publish/subscribe messaging and data persistence for containers.

- **Runtime support:** we have developed a framework based on the MAPE-K [9] loop to automatically monitor, execute the expected behaviour and self-adapt the IoT system by executing the IoT execution rules modeled with the DSL, including rules for the self-adaptation of the system to ensure its QoS.
- **Code generator enhancements:** We now generate the code required to support the execution of the whole system at runtime (including the code for infrastructure monitoring and system management tools).
- **a DSL extension for the mining industry:** we propose an extension of our DSL focused on the modeling and operation of IoT systems in the underground mining industry, highlighting the ability to reuse the DSL in other domains.
- **Empirical evaluations:** we have designed and conducted empirical experiments to validate the expressiveness and usability of our DSL and the correctness of the generated code.

The remainder of the paper is organized as follows: Section 2 presents a running example to illustrate our approach. Section 3 introduces the DSL to specify multi-layered IoT systems and adaptation rules. Section 4 present an extension of our DSL for IoT systems deployed in underground mining. In Section 5, we present the DSL implementation, the framework to support IoT systems at runtime, and code generation. In Section 6, we validate the usability of our DSL and the generated runtime. Finally, the related work to this research is summarized in Section 7, and the conclusions and future work are presented in Section 8.

2 Running Example

We will use a Smart Building scenario as a running example to illustrate our approach. Smart buildings seek to optimize different aspects such as ventilation, heating, lighting, energy efficiency, etc [10].

For the purposes of our example, let's assume that a hotel company (*Hotel Beach*) wants to reduce fire risks by automating disaster management in its hotels. A fire alarm and monitoring system are implemented in each of the company's hotels. We will assume that all buildings (hotels) have three floors with two rooms each. Fig. 1 presents an overview of the 1st floor. Based on this, the infrastructure (device, edge, and cloud layers) of the company hotel IoT system would be as follows:

- **Device layer.** Each room has a temperature sensor, a carbon monoxide (CO) gas sensor, and a fire water valve. Furthermore, an alarm is deployed on the lobby. Each sensor has a threshold measurement to activate the corresponding alarm, e.g., a person should not be continuously exposed to CO gas level of 50 parts per million (ppm) for more than 8 hours.
- **Edge layer.** In each room, an edge node receives the information collected by the sensors of the device layer and run a software container (C1 and C2) for analyzing sensor data in real time to check for the presence of smoke and generate an alarm state that activates the actuators. A fog node (linked to

4 *A model-based infrastructure for self-adaptive IoT architectures*

the edge nodes), located in this same floor, runs the C3 container (running App2, a machine learning model to predict fires), and C4 (running App3, in charge of receiving and distributing data, typically a Message Queuing Telemetry Transport (MQTT)).

- **Cloud layer.** The cloud layer has a cloud server node that runs the C5 container, a web application (App4) to display historical information of sensor data and of fire incidents in any of the hotel's property of the company.

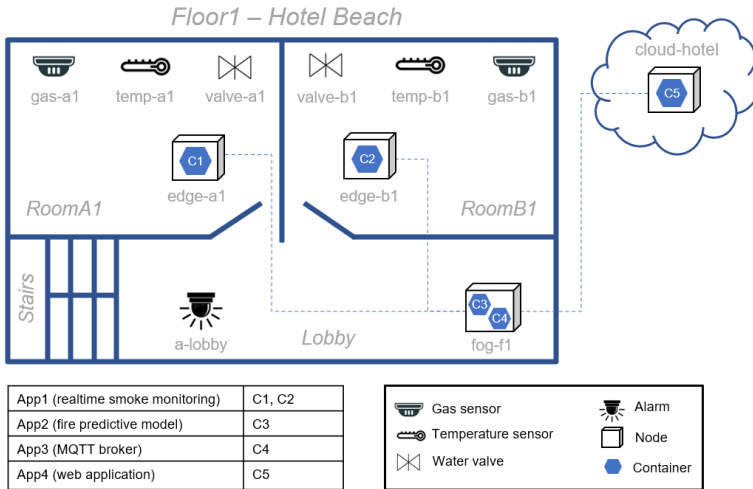


Fig. 1: Overview of the smart building IoT system, first floor

This covers the static view of the system. But in any IoT system, there are critical applications that should be available all the time. For example, the availability of the containers running App1 (real-time smoke monitoring) should be guaranteed. However, some environmental factors can impact their availability. In these cases, the IoT system must self-adapt to guarantee its operation. For instance, a flooding could cause failures in the *edge-a1* node; then it will be necessary to migrate the *C1* container to another suitable node to ensure the continuous monitoring of the smoke presence.

Our research addresses this type of architectural adaptations by proposing a rule-based language for the runtime execution of IoT systems that can also be used to address their functional requirements. An example of this latter case would be a rule stating that when one of the room sensors detects CO gas greater than 400 ppm, an of the alarms should be triggered. The next section shows how we can model all these concepts.

3 A DSL for the specification of multi-layered IoT systems

A DSL is defined by three core ingredients [3]: the abstract syntax (i.e., the concepts of the DSL and their relationships), the concrete syntax (the notation

to represent those concepts), and its semantics which are hardly ever formalized but based on the shared understanding of the domain. In this chapter, we present our DSL for modeling multi-layered IoT architectures (section 3.1) and their dynamic (3.2) rules.

3.1 Modeling the IoT Architecture

Traditionally, IoT system architectures consisted of two layers: device and cloud [11]. The device layer is composed by sensors (devices that sense physical properties such as temperature and humidity), actuators (devices such as valves, fans, or alarms that can influence an automated process), and network devices that send data to the cloud layer, composed of servers that run the application logic. Today, multi-layered architectures based on edge and fog computing have emerged to increase the flexibility of pure cloud deployments and help meet non-functional IoT system requirements [12].

There are several definitions for edge and fog computing. [13] states that edge computing enables computations to be performed at the edge, supporting cloud and IoT services. On the other hand, [14] defines fog computing as a bridge between the cloud and the edge of the network to facilitate the deployment of new IoT applications providing computation, storage, and network services. There are strong similarities between these two concepts, but the main difference is where the processing takes place. While fog computing take place on LAN-connected nodes usually close to end user devices, edge computing takes place on personal devices directly connected to sensors and actuators, or on gateways physically close to these [14, 15].

Edge and fog computing can leverage containerization as a virtualization technology [16]. Containers, compared to virtual machines, are lightweight, simple to deploy, support multiple architectures, have a short start-up time, and are suitable for dealing with the heterogeneity of edge and fog nodes. In terms of communications, asynchronous message-based architectures are typically chosen, especially for IoT systems that require high scalability [17]. The publisher/subscriber pattern and the MQTT protocol are becoming the standard for Machine-to-Machine communications [18], where messages are sent (by publishers) to a message broker server and routed to destination clients (subscribers).

Our DSL enables the specification of all these concepts.

3.1.1 Abstract syntax

The abstract syntax of a DSL is commonly defined through a metamodel that represents the domain concepts and their relationships. Fig. 2 shows our metamodel that abstracts the concepts required to define multi-layered IoT architectures.

The sensors and actuators of the device layer are modeled using the *Sensor* and *Actuator* concepts that inherit from the *IoTDevice* concept. All *IoTDevices* have a connectivity type (such as Ethernet, Wi-Fi, ZigBee, or another).

The location of *IoTDevices* can be specified through geographic coordinates (*latitude* and *longitude* attributes). Moreover, *Sensors* and *Actuators* have a type represented by the concepts *SensorType* and *ActuatorType* to organize different sensors belonging to the same category and be able to define global rules for them. For instance, following the running example (Fig. 1), there are temperature and smoke type sensors, and there are valve and alarm type actuators. We also cover the concepts for specifying MQTT communications: *IoTDevices* are publishers or subscribers to a topic specified by the relationship to the *Topic* concept. The gateway of an *IoTDevice* can be modeled through the *gateway* relationship with the *EdgeNode* concept. Via this gateway, the sensor can communicate with other nodes, e.g., the MQTT broker node. Additionally, the threshold value and unit of the monitored variable by a sensor can be represented through the attributes *threshold* and *unit*.

Physical (or even virtual) spaces such as rooms, stairs, buildings, or tunnels can be represented by the concept *Region*. A *Region* can contain subregions (relationship *subregions* in the metamodel). For example, region *Floor1* (Fig. 1) contains subregions *Room1*, *Room2*, *Lobby*, and *Stairs*. *IoTDevices*, *EdgeNodes*, and *FogNodes* are deployed and are located in a region or subregion (represented by *region* relationships in the metamodel). Back to the running example, the *edge-a1* node is located in the *RoomA1* region of *Floor1* of the *Hotel Beach*, while the *fog-f1* node is located in the *Lobby* region of *Floor1*.

Edge, fog and cloud nodes are all instances of *Node*, one of the key concepts of the metamodel. Communication between nodes can be specified via the *linkedNodes* relationship, as we may want to indicate what nodes on a certain layer could act as reference nodes in another layer. Nodes can also be grouped in clusters that work together. A *Node* can host several software containers according to its capabilities and resources (primarily *cpuCores*, *memory*, and *storage*). The CPU and memory usage of a container can be restricted through *cpuLimit* and *memoryLimit* attributes. Each software container runs an application (represented by the concept *Application*) that has a minimum of required resources specified by the attributes *cpuRequired* and *memoryRequired*. The repository of the application image is specified through the *imageRepo* attribute. The container volumes and their paths (a mechanism for persisting data used and generated by containers) are represented by the *Volume* concept.

3.1.2 Concrete syntax

The concrete syntax refers to the type of notation (such as textual, or graphical) to represent the concepts of the metamodel. Graphical DSLs involve the development of models using graphic items such as blocks, arrows, axes, and so on. Textual DSLs involve modeling using configuration files and text notes. Though most DSLs employ a single type of notation, they could benefit from offering several alternative notations, each one targeting a different type of DSL user profile. This is the approach we follow here, leveraging the benefits of using a projectional editor.

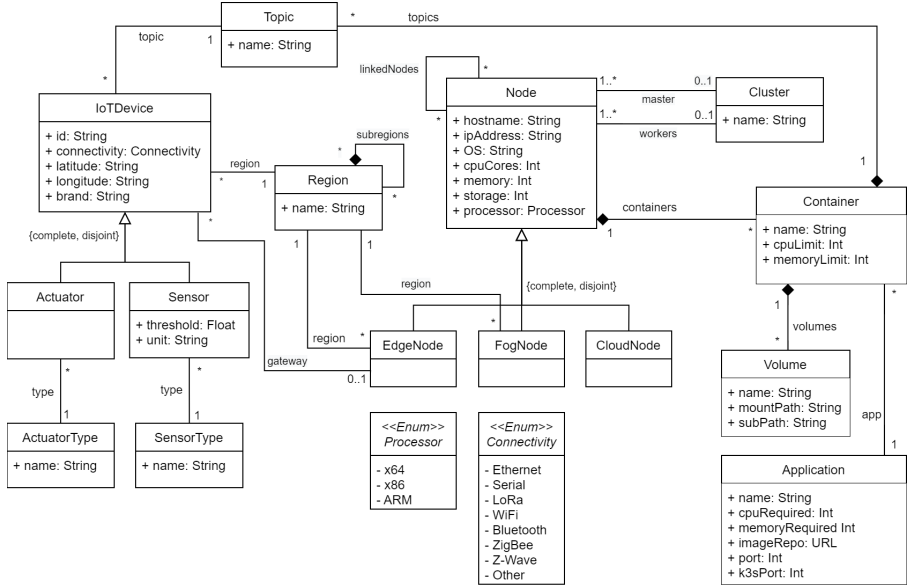


Fig. 2: Multi-layer IoT architecture metamodel

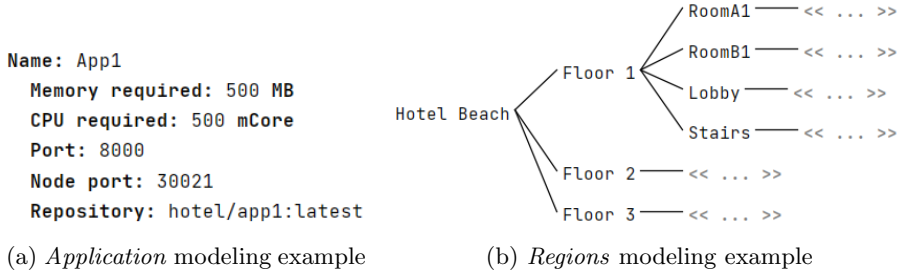
Projectional editors enable the user’s editing actions to directly change the Abstract Syntax Tree (AST) without using a parser [19]. That is, while the editing experience simulates that of classical parsing-based editors, there is a single representation of the model stored as an AST and rendered in a variety of perspectives thanks to the corresponding projectional editors that can deal with mixed-language code and support various notations such as tables, mathematical formulas, or diagrams.

Indeed, we take advantage of JetBrains Meta Programming Systems (MPS) projectional editors to define a set of complementary notations for the meta-model concepts. We blend textual, tabular, and tree view, depending on the element to be modeled. We next employ these notations to model our running example (Section 2). More technical details on the implementation of our concrete notations are presented in Section 5.

3.1.3 Example scenario

We present next how to model the IoT architecture of the running example (Section 2) using our DSL. First, Fig. 3a depicts the modeling of the application *App1*, including its technical requirements and repository address. Then, Fig. 3b shows the specification of the *Hotel Beach* regions, in particular those on *Floor 1* (four subregions: two *Rooms*, the *Lobby* and the *Stairs*).

Additionally, *IoT devices* can be modeled using a tabular notation. Fig. 4 shows the list of sensors and actuators located in the *RoomA1* region (we have omitted some parameters for readability purposes). To specify the nodes of the system architecture, we propose a tabular notation as well (Fig. 5 shows

**Fig. 3:** *Application* and *Regions* modeling example

edge-a1 and *fog-f1* node modeling). The node description includes the layer it belongs to, the hardware properties, the regions where it is located, and the hosted application containers. Each container includes the specification of the application to be executed, limits, and volumes (e.g., the volume of the *C4* container for the configuration of the MQTT broker).

	Device	ID	Type	Unit	Threshold	Regions	Brand	Communic.	Gateway	Topic
1	Sensor	gas-a1	C0	ppm	50	RoomA1	Winsen	ZigBee	edge-a1	f1/rA1/smoke
2	Sensor	temp-a1	Temperature	°C	23	RoomA1	MLX	Z_Wave	edge-a1	f1/rA1/temp
3	Actuator	valve-a1	Valve	---	---	RoomA1	Bray	Serial	edge-a1	f1/rA1/valve

Fig. 4: IoT devices modeling example (tabular notation)

	Hostname	Layer	Properties	Regions	Linked nodes	Containers
1	edge-a1	Edge	Memory: 2000 MB Storage: 16000 MB CPU cores: 1 Core IP address: 192.168.10.1 Operating system: Raspbian Processor: ARM	RoomA1	fog-f1	* Name: C1 Application: App1 Memory limit: no limit CPU limit: no limit Volumes: << ... >>
2	fog-f1	Fog	Memory: 4000 MB Storage: 20000 MB CPU cores: 2 Cores IP address: 192.168.10.3 Operating system: Raspbian Processor: ARM	Lobby	cloud-hotel	* Name: C3 Application: App2 Memory limit: no limit CPU limit: no limit Volumes: << ... >> * Name: C4 Application: App3 Memory limit: no limit CPU limit: no limit Volumes: -> Name: mosquitto-config Mount path: /config/mqtt.conf Sub path: mosquitto.conf

Fig. 5: Nodes and containers modeling example (tabular notation)

3.2 Modeling Dynamic Rules

The dynamic environment of an IoT system requires dealing with expected an unexpected events. The former may trigger actions to comply with the

standard behaviour of the system (e.g. to turn on an alarm upon detection of fire), unexpected ones may require a self-adaptation of the system itself to continue its normal operation. This section presents a rule-based language that can cover both types of events (and even mix them in a single rule). This facilitates an homogeneous of all the dynamic aspects of an IoT system.

To decide what unexpected environmental situation should we include and what the standard patterns of response are common in the self-adaptation of IoT systems, we rely on our previous systematic literature review [11]. For instance, the three architectural adaptations (offloading, scaling, and redeployment) addressed in this study were identified in the SLR. Our language covers all of them and even enables complex rules where policies involving several strategies can be attempted in a given order.

3.2.1 Abstract syntax

The metamodel representing the abstract syntax for defining the rules is depicted in Fig. 6.

Every rule is an instance of *Rule* that has a triggering condition, which is an expression. We reuse an existing *Expression* sublanguage to avoid redefining in our language all the primitive data types and all the basic arithmetic and logic operations to manipulate them. Such Expression language could be, for instance, the Object Constraint Language (OCL), but to facilitate the implementation of the DSL later on, we directly reused the MPS *Baselanguage*. The metamodel extends the generic Expression concept by adding sensor and QoS conditions that can be combined also with all other types of expressions (e.g., numerical ones) in a complex conditional expression.

A *SensorEvent* represents the occurrence of an event resulting from the analysis of sensor data (e.g., the detection of dioxide carbon gas by the *gas-a1* sensor). Note that *SensorEvent* conditions can be linked to specific sensors or to sensor types to express conditions involving a group of sensors.

Similarly, the *QoSEvent* condition is a relational expression that represents a threshold of resource consumption or QoS metrics. This condition allows checking a *Metric* (such as Latency, CPU consumption, and others) on a specific node or a group of nodes belonging to a *Region* or *Cluster*. For example, the condition *cpu(HotelBeach- > edge_nodes) > 50%* is triggered when the CPU consumption on the edge nodes of the *Hotel* exceeds 50%.

Moreover, we can define that the condition should be true over a certain period (to avoid firing the rule in reaction to minor disturbances) before executing the rule. Once fired, all or some of the actions are executed in order, depending on the *allActions* attribute. If set to false, only the number of *Actions* specified by the attribute *actionsQuantity* must be executed, starting with the first one in order and continuing until the required number of actions have been successfully applied.

For the sake of clarity, we have grouped the rule concepts into two categories: *Architectural Adaptation Rules* and *Functional Rules* but note that they could be all combined, e.g., a sensor event could trigger at the same time

a functional response such as triggering an alarm and, at the same time, an automatic self-adaptation action, such as scaling of apps related to the event to make sure the IoT system has the capacity to collect more relevant data).

Among the self-adaptation patterns, the *Offloading* action consists in migrating a container from a source node to a destination node. This migration can be among nodes of different layers. The *container* relationship represents the container that will be offloaded. The target node is specified by the *targetNode* relationship. However, if the target node does not have the resources to host the container, a cluster or a group of nodes in a *Region* can be specified (*targetRegion* and *targetCluster* relationships) to offload the container. The *Scaling* action involves deploying replicas of an application. This application is represented by the *app* relationship, and the number of replicas to be deployed is defined by the *instances* attribute. The replicas of the application are deployed in one or several nodes of the system represented by the *targetNodes*, *targetCluster*, and *targetRegion* relationships. The *Redeployment* action consists in stopping and redeploying a container running on a node. The container to redeploy is indicated by the *container* relationship. Finally, the *OperateActuator* action is to control the actuators of the system (e.g., to activate or deactivate an alarm). The message attribute represents the message that will be published in the broker and interpreted by the actuator.

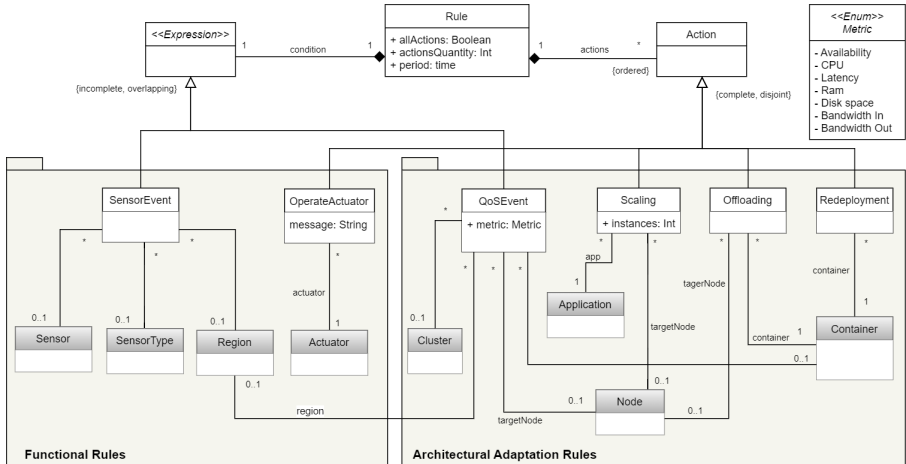


Fig. 6: IoT system dynamic rules metamodel

3.2.2 Concrete syntax

Rules are specified thanks to a textual notation using as keywords the names of the metaclasses of the abstract syntax. The conditions follow the grammar of a relational expression with the use of mathematical symbols (such as $<$, $>$, and $=$) and logical operators (such as $\&$ and \parallel). The rule editor (see Section

5) offers a powerful autocomplete feature to guide the designer through the rule creation process.

3.2.3 Example Scenario

We show how to use the rule's concrete syntax to model two example rules from the smart building example.

First, to guarantee the execution of the *C4* container deployed on the *fog-f1* node, we modeled the rule as shown in (Fig. 7a). This rule offloads the container *C4* hosted on node *fog-f1* to a nearby node (e.g., node *edge-b1*) when the CPU consumption exceeds 80% for one minute. If the *edge-b1* node does not have the necessary resources to host that new container (when the rule is activated), a Region (e.g., *Floor1*) can be specified so that a suitable node will be searched there. However, if this offloading action cannot be executed, for example, because in *Floor1* there is no node capable of hosting the container, then we must define a backup action. Therefore, we have modeled a second action (*Scaling*) to deploy a new container instance of the *App3* application on any of the nodes of the *Hotel Beach*. When a list of actions is specified, the checkbox *all actions* controls whether all or only a certain number of them should be performed. All actions in the list will be performed. For *Rule 1*, only one action (the first one, or the second one if the first one fails) will be executed.

Secondly, we model another rule (see Fig. 7b) to activate the alarm (*a-lobby*) when any gas sensors in the *Floor1* region (gas-a1 or gas-b1) detects a gas concentration greater than 400ppm for 10 seconds. The "On" message is published in the broker topic consumed by the actuator (*a-lobby* alarm). Note that there are two ways to model this rule. While Option 1 involves all CO type sensors on *Floor 1*, Option 2 directly involves both gas sensors.

Rule 1 Condition: (cpu[fog-f1]) > (80 %) Period: 1 m Actions: <input type="checkbox"/> all actions 1 * Offloading -> Container: C4 Target node(s): edge-b1 Target region(s): Floor 1 * Scaling -> Application: App3 Instances: 1 Target node(s): << ... >> Target region(s): Hotel Beach	Rule 2 - option 1 Condition: (Floor 1 -> CO) > (400 ppm) Period: 10 s Actions: * Operate Actuator -> Actuator: a-lobby message: On Rule 2 - option 2 Condition: (gas-a1) > (400 ppm) (gas-b1) > (400 ppm) Period: 10 s Actions: * Operate Actuator -> Actuator: a-lobby message: On
(a) Rule 1 modeling	(b) Rule 2 modeling

Fig. 7: Example of rule modeling

4 DSL Extension: Coal Underground Mining

Our DSL can be used as is to model any type of multi-layered IoT system. However, it has also been designed to be easily extensible to further tailor it to specific types of IoT systems. As an example, we present an extension of our DSL to model underground mining systems as this is a key economic sector in the local region of one of the authors and there is a need for a better modeling of these systems, e.g., for analysis of regulatory compliance.

Indeed, the dynamic and hostile environment of the underground mining industry threatens the operation of IoT systems (e.g. by causing physical damage to the devices) implemented primarily to monitor and ensure the safety of workers. Explosive and toxic gases, risk of geotechnical failure, fire, high temperatures and humidity are some of the risks. Therefore, mining IoT systems must cope with these unexpected changes by self-adapting to guarantee a proper run-time operation.

In addition to system self-adaptations, our DSL should support expressing mining functional requirements. For example, in Colombia, the safety regulation for underground mining works (decree 1886 of 2015) determines limits for the concentration of explosive and toxic gases. If any of these limits is exceeded, a series of actions/adaptations must be performed such as turning on alarms, activating the ventilation system, etc.

To better cope with these scenarios, our extended DSL offers new modeling primitives (see Figure 8). All concepts that inherit from *Region* represent physical spaces. A *Tunnel* can be *Internal* or *Access*. Each mine access tunnel (*Drift*, *Slope*, or *Shaft*) must have one or more entrances (represented by the *entries* relationship). Finally, checkpoints (areas of the mine where gases, temperature, oxygen, and airflow are monitored) are specified through the *CheckPoint* concept. Each *CheckPoint* could contain multiple *IoTDevices* (sensors or actuators) represented by the *devices* relationship in the metamodel.

We offer a tree-based notation for modeling the relevant regions¹ that make up the mine structure. Figure 9 presents an example of the modeling of an underground mine containing two entries (*Entry A* and *Entry B*) in each of its inclined access tunnels (*Slope A* and *Slope B*), an internal tunnel (*Internal*), and a (*Room*) with two exploitation work fronts (*W-front 1* and *W-front 2*).

At each mine control point, the airflow should be controlled by the fans. While very fast air currents can produce fires, very low air currents may not be efficient in dissipating gas concentrations. To involve control points directly in the adaptation rules, we have also modified our language. This extension of the DSL enables the modeling of conditions such as (*ControlPointA* \rightarrow *airFlow*) > (2m/s).

All the other concepts directly reuse the notation of the core DSL presented in Section 3.

¹Note that our DSL is focused on the structure and rules governing the “behaviour” of the IoT system of the mine, it does not pretend to replace other types of 3D mine mining models

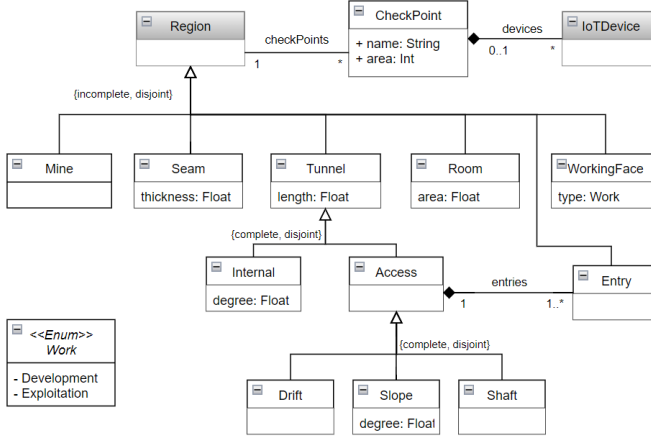


Fig. 8: Excerpt of the DSL extension metamodel

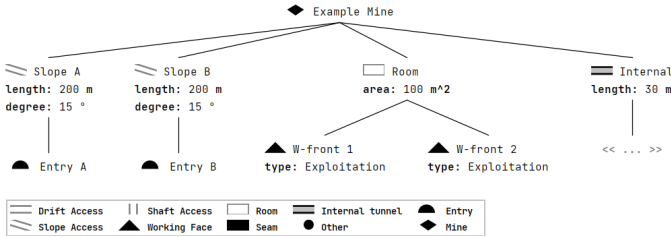


Fig. 9: Mine structure modeling

5 Tool Support

In this section, we describe the implementation and tool support for both our DSL and the core runtime framework responsible for monitoring and self-adapting IoT systems at runtime. Once both are described, we discuss the link between the two, i.e. the code generator that takes as input the model specified with our DSL and generates the code for runtime deployment and execution of the system.

5.1 DSL Tool Support

Our DSL is created using MPS, an open-source language workbench developed by JetBrains. By building the DSL on top of MPS, we automatically get a projectional editor for the DSL with facilities the implementation of the different notations highlighted in the previous sections. The DSL editor is freely available in our repository [20].

In particular, to develop the modeling environment for the DSL, we had to define in MPS three core elements: *structure*, *editors* and *constraints*. The

structure is equivalent to the abstract syntax of the DSL. Projection editors define the desired Abstract Syntax Tree (AST) code editing rules. For our DSL We have defined textual, tabular, and tree view editors by implementing the mbeddr² extension of MPS.

For example, Fig. 10 shows the definition of the tabular editor for modeling the *Sensor* concept. We have used the *partial table* command to define the table structure (cells, content, and column headers). By defining this editor, the user is enabled to model *Sensors* using a tabular notation as shown in Fig. 4.

```

tabular editor for concept Sensor
node cell layout:
  partial table {
    horizontal r<> {
      cell Sensor c<"Device"> r<>
      cell { name } c<"ID"> r<>
      cell ( % type % -> { name } ) c<"Type"> r<>
      cell { unit } c<"Unit"> r<>
      cell { threshold } c<"Threshold"> r<>
      cell
      ( / % regions %  / ) c<"Regions"> r<>
      /empty cell: <default> 
      cell { brand } c<"Brand"> r<>
      cell { communication } c<"Communic."> r<>
      cell ( % gateway % -> { name } ) c<"Gateway"> r<>
      cell ( % topic % -> { name } ) c<"Topic"> r<>
      cell { latitude } c<"Latitude"> r<>
      cell { longitude } c<"Longitude"> r<>
    }
  }

```

Fig. 10: Definition of the tabular editor for the *Sensor* concept

Finally, constraints restrict the relationships between nodes as well as the allowed values for properties. We have used this constraint mechanism to embed in the editor several well-formedness rules required in our DSL specification. For instance, we have added constraints to avoid repeated names, constraints to limit the potential values of some numerical attributes, constraints to restrict the potential relationships between nodes, and other constraints that prevent ill-formed models from being built.

5.2 Runtime Tool Support

Figure 11 summarizes an operational view of our architecture by distinguishing design time (left-hand side) and runtime (right-hand side).

At design time, the user creates an initial IoT system specification model using the modeling editor for the DSL described in the previous section. The code generator, presented in Section 5.3, transforms such a specification into a set of deployment and configuration options that describe a MAPE-K loop [9]

²<http://mbeddr.com/>

which is performed at runtime. This section covers these components so that we can then describe in the next section how they are generated from the DSL definition.

The MAPE-K loop is a reference model to implement adaptation mechanisms in auto-adaptive systems. This model includes four activities (monitor, analyze, plan, and execute) in an iterative feedback cycle that operate on a knowledge base (see Figure 11). These four activities produce and exchange knowledge and information to apply adaptations due to changes in the IoT system.

Based on the MAPE-K loop, our runtime architecture is composed of a set of components and technologies to monitor, analyze, plan, and execute adaptations as illustrated in the right-hand side of Figure 11). We next describe how our architecture particularizes the generic MAPE-K concepts for self-adaptive IoT systems.

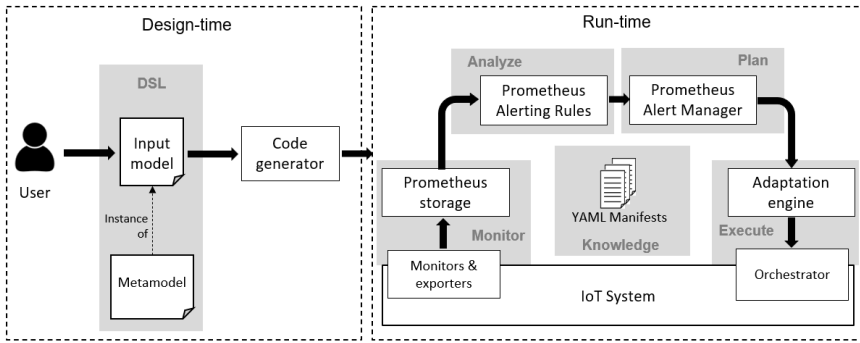


Fig. 11: Overview

5.2.1 Monitor

In the monitoring stage, information about the current state of the IoT system is collected and stored. The collected information is classified into two groups: (1) infrastructure and QoS metrics (presented in Table 1); and (2) information that is published in the system's MQTT broker topics such as temperature, humidity, gas levels, and other types of sensor data. These two kinds of information are aligned with the addressed types of events to be detected, i.e., QoS events and sensor events.

We have implemented Prometheus Storage³ (a time-series database) to store the information collected by the exporters and monitors (such as *kube-state-metrics*⁴ and *node-exporter*⁵). Exporters are deployed to convert existing metrics from third-party apps to Prometheus metrics format. The information

³<https://prometheus.io/docs/prometheus>

⁴<https://github.com/kubernetes/kube-state-metrics>

⁵<https://github.com/prometheus/node-exporter>

collected and stored can be queried in real time through the Prometheus user interface or the Grafana dashboard.

Table 1: QoS and Infrastructure metrics

Metric	Exporter	Description
Availability	Kube-state-metrics	Equal to 1 if the component being monitored is available, 0 otherwise
CPU	Node Exporter	Number of seconds the CPU has been running in a particular mode
RAM	Node Exporter	Available and total Ram memory of the node
Disk usage	Node Exporter	Available and total disk space of the node
Bandwidth in	Node Exporter	Number of bytes of incoming network traffic to the node
Bandwidth out	Node Exporter	Number of bytes of outgoing network traffic from the node

5.2.2 Analyze

The information collected in the monitoring phase must be analyzed, and changes in the system that require adaptations must be identified. To deal with this, we have implemented Prometheus Alerting Rules to define alert conditions based on Prometheus query language expressions (PromQL) and to send notifications about firing alerts to the next MAPE-K loop phase. Each IoT system rule specified through the DSL is transformed into an alert rule of Prometheus.

5.2.3 Plan

According to the analysis made in the previous stage, an adaptation plan is generated with the appropriate actions to adapt the system at runtime. The adaptation plan contains the list of actions (scaling, offloading, redeployment, and operate actuator) that the user has defined for each rule via the DSL. In this stage, Prometheus Alert Manager is used to handle the alerts from the previous stage (Analyze) and routing the adaptation plan to the next stage (Execute). The adaptation plan is sent as an HTTP POST request in JSON format to the configured endpoint (i.e., to the Adaptation Engine).

5.2.4 Execute

In the Execute stage, the actions are applied to the IoT system following the actions defined in the adaptation plan. To achieve this, we have built an Adaptation Engine, an application developed using Python, flask, and the python API to manage the Kubernetes orchestrator. The adaptation engine can apply two sets of actions: (1) architecture adaptations through the orchestrator (e.g., autoscaling an application or offloading a pod); and (2) regular system operations such as controlling a system actuator by sending it an instruction (e.g., a

message to turn on or off an alarm). This adaption is generic and can be used to run any IoT system modeled with our DSL, including its mining extension.

5.2.5 Putting it all together: Example scenario

To better understand how the different elements cooperate, we will exemplify how the framework monitors and executes the rule specified in Figure 7a. Code for the rule management is automatically generated (Section 5.3), including YAML⁶ manifests for deployment, configuration and execution of the monitors, exporters, Prometheus, the Adaptation Engine and other software components implemented in the MAPE-K loop.

In the Monitoring stage, the exporters gather information about CPU consumption of the *fog-f1* node. This information is stored in the Prometheus database. Then, in the Analysis stage, the condition of the rule is verified by executing query expressions in PromQL language. For example, the expression (executed by Prometheus Alerting Rules) that checks if the CPU consumption of the fog-f1 node exceeds 80% for 1 minute is presented in listing 1. Note that we are calculating the average amount of CPU time used excluding the idle time of the node. If the condition is true, the alert signal is sent to the Alert Manager component of the next stage of the cycle (Plan). When the alert is received, the adaptation plan is built containing the two actions (offloading and scaling) and their corresponding information such as container to be offloaded, application to be scaled, number of instances, target nodes and target regions. In the Execute stage, the Adaptation Engine component first performs the Offloading action, and only if it fails, then the second action (Scaling) is performed.

```

1  - alert: ram-consumption
2    expr: 100 - (avg by(node_hostname) (rate(node_cpu_seconds_total{mode=
      "idle",node_hostname="fog-f1"}[15s])) * 100) > 80
3    for: 1m

```

Listing 1: Query expression to check CPU consumption of fog1-f1 node

5.3 Code Generator

To configure and run the runtime infrastructure of an IoT system from its DSL model, we have implemented a model-to-text transformation that generates YAML files to deploy the IoT system's container-based applications and the components of each stage of our MAPE-K loop based framework, including its internal logic. In particular, the generated code includes the following components:

- The container-based IoT applications specified in the input model. Following the running example of Section 2, the YAML manifests for deployment of containers C1, C2, C3, C4, and C5 are generated
- YAML Manifests to deploy the monitoring tools and exporters such as kube-state-metrics, node-exporter, and mqtt-exporter

⁶YAML is a data serialization language typically used in the design of configuration files

- YAML code to deploy and configure the Prometheus Storage, Prometheus Alerting Rules, and Prometheus Alert Manager components. The PromQL code to define the rules (e.g., the code shown in Listing 1) is also generated as a Prometheus configuration file
- YAML manifest to deploy the Adaptation Engine
- and the Grafana application to display the monitored data stored in the Prometheus database.

Due to space limitations, we do not show here the model-to-text transformation. You can find all this information in the project repository [20], including the generated code for the running example from Section 2.

6 Empirical Evaluation

We have designed and conducted three experiments to validate our DSL and its accompanying infrastructure.

6.1 Language Validation

We conducted two experiments to validate the expressiveness and ease of use of our DSL: *Experiment 1*, focused on specific mining concepts, and *Experiment 2*, focused on core architectural concepts, both based on the basic methodology for conducting usability studies [21]. Both also cover the modeling of adaptation rules.

We report here the results of *Experiment 1*. Full details of *Experiment 2* are available on the project repository⁷).

6.1.1 Experiment design and setup

We designed the experiment to validate the expressiveness and usability of the DSL regarding the modeling of the mine structure, the control points, sensors and actuators, and rules to manipulate such actuators (e.g., turn on the mine ventilation system when the methane gas sensor exceeds the threshold value).

Eight subjects participated in the experiment. Participants were experts from the mining domain, but had not been exposed to our DSL before. The goal was to check whether they were able to use it and get their feedback on the experience.

The experiment consisted of an asynchronous screening test (pre-questionnaire) to assess subjects' prior knowledge and suitability for participation, and a synchronous exercise (virtual meeting) with two parts (Sessions 1 and 2). The materials and exercises provided to the participants, the questionnaires and the anonymized answers can be found in the repository of our DSL extended to the mining industry domain⁷.

- Pre-questionnaire (10 min): this screening questionnaire (Q0) was conducted prior to the start of Sessions 1 and 2 to ensure that participants had a basic

⁷<https://github.com/SOM-Research/IoT-Mining-DSL>

level of mining knowledge including the structure of underground coal mines, gas monitoring systems, and modeling tools in this domain.

- Session 1 (50 min): In the first 20 minutes, we introduced basic knowledge of IoT systems and the use of the DSL implemented in MPS to model the structure of underground mines, the control points and the IoT devices deployed (sensors and actuators). Next, the participants performed the first modeling exercise about an underground coal mine (with the structure shown in Figure 9), two control points (one at each working face) with three gas sensors and an alarm, a fan, and a control door in the internal tunnel. Each participant was provided with a virtual machine configured with the necessary software to perform the modeling exercise. Finally, the participants filled out a questionnaire (Q1) about the usability and expressiveness of the DSL to model the concepts of the first exercise.
- Session 2 (40 min): In Session 2, we first introduced the basic concepts of self-adaptive systems and the design of rules using our DSL. Next, participants performed the second exercise: modeling three rules involving sensor data and actuator operation. For example, if any of the methane gas sensors throughout the mine exceed the threshold value for 5 seconds, then turn on the fan and activate the alarms. Finally, participants completed the questionnaire Q2 to report their experience modeling the rules. Q2 also contained open-ended questions to obtain feedback on the use of the entire tool and suggestions for improvement.

The experiment was conducted in Spanish on three different dates in 2022. The first author of the paper conducted the virtual meetings and ensured that all were equally well executed.

6.1.2 Results

Four of the participants were involved in education (either students, teachers, or researchers), while the remaining four were involved in industry. All of them are aware of the terminology used in the design and structure of underground coal mines. Only two participants were not familiar with cyber-physical or IoT systems for mining. The modeling tools in mining context that they have used are AutoCAD⁸ and Minesight⁹ for the graphical design of the mine structure, and VentSim¹⁰ for ventilation system simulations. None of them were familiar with MPS.

Figure 12a presents the responses from questionnaires Q1 and Q2 related to the ease of use of the DSL. Most of them reported that the modeling of the mine structure, the control points, the devices (sensors and actuators), and the rules were easy. The results are positive and can also be evidenced by the number of right and wrong concepts modeled by the participants (Figure 12b). The number of errors were low (12 of 188 modeled concepts): three incorrect *Rule-conditions* by wrong selection of the unit of measure, four incorrect *Actuators*

⁸<https://www.autodesk.com/products/autocad>

⁹<https://its.mines.edu/software-title/minesight/>

¹⁰<https://ventsim.com>

by wrong assignment of actuator type and location within the mine, three missing *Sensors* not modeled, and two incorrect *Regions* (working faces) whose type was not selected.

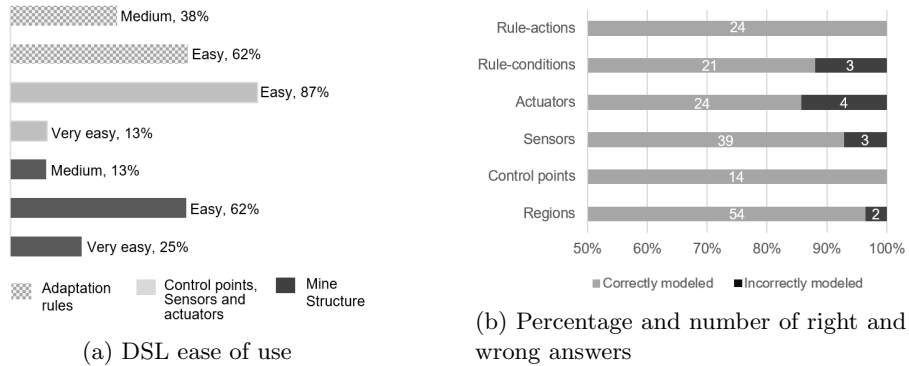


Fig. 12: Validation results

Through the open-ended questions in questionnaires Q1 and Q2, participants suggested the following improvements to the DSL.

- Include the specification of the coordinates for each region and control points of the mine. Additionally, it would be useful to specify the connection between internal tunnels.
- The condition of a rule has a single time period. However, it would be useful to associate two time periods for conditions composed of two expressions. For example, the condition $tempSensorA > 30C(10seconds) \ \&\& \ tempSensorB > 35C(20seconds)$.
- The mine ventilation system can be activated periodically at the same time each day. It would be useful if the DSL could model rules whose condition is associated with the time of day.

6.1.3 Threats to Validity

Although validation problems in empirical experiments are always possible, we have looked for methods to ensure the quality of the results, analyzing two types of threats: internal and external.

Internal validation concerns factors that could affect the results of the evaluation. To avoid defects in the planning of the experiments and the questionnaires (protocol), all authors of the paper discussed the protocol including the modeling exercises, the dependent variables, and the questions of the questionnaires. In addition, a senior researcher (not in the authors list) in empirical experiments validated the questionnaires. Another common thread is related to the low number of samples to successfully reveal a pattern in the results.

Thirteen users total participated in this empirical validation. Eight participants were involved in Experiment 1, and five different ones in Experiment 2. Although the size of the participant group for this type of validation continues to be a matter of discussion, studies suggest 3 to 10 participants (depending on the level of complexity) are sufficient. For example, a popular guideline in this area is given by Nielsen and Landauer [22], who suggest that five participants are likely to discover 80% of the problems.

External validity addresses threats related to the ability to generalize results to other environments. For example, to validate the population and avoid sampling bias, we conducted a pre-questionnaire to the participants to ensure that they had the necessary basic knowledge and that there was no substantial difference between participants. In addition, at the beginning of each session, we introduced the definition of the concepts required for the experiment. It is important to emphasize that the participants of Experiment 1 were related to the topics of the mining domain, while those of Experiment 2 were computer science researchers.

6.2 Runtime Framework Validation

To evaluate the self-adaptation capability of our approach and the correctness of the code-generation and runtime infrastructure, we conducted experiments to test the architectural adaptations (scaling, offloading, and redeployment).

For each adaptation assessment we have designed a simple scenario in which an IoT system faces an event that forces adaptations. We have validated that starting from the IoT model including a specified rule triggered by such event, the code-generator creates the deployment infrastructure to run the IoT system and assess that such system actually adapts as expected when the event is triggered. We have collected and analyzed metrics such as CPU consumption, node availability, and time spent in each stage of the MAPE-K loop to also show the benefits of such self-adaptive architecture when the system is under pressure.

The design of these experiments and the results are in the appendices of the paper that can be found in the project repository [20].

7 Related Work

Modeling of cloud architectures has been widely studied, including provisioning of resources for cloud applications. Nevertheless, most proposals do not cover multi-layered architectures involving fog and edge nodes. This is also the case for Infrastructure-as-code (IaC) tools.

Some works such as [23–25] focus on the cloud layer. Others, like [5–7] are oriented towards the edge and fog layers. In particular, studies such as [5, 6] focus on the modeling of sensors, actuators, and software functionalities, while [7] addresses the modeling of application deployment at the fog layer. Works like [26, 27] are oriented towards lower-level communication aspects and individual IoT component behaviours.

A few proposals are closer to ours in terms of the static modeling of IoT systems, such as [28, 29] but using less expressive DSLs and, especially, limited possibilities when it comes to the definition of rules, including self-adaptive ones.

Indeed, support for (self-adaptive) rules is less covered by previous approaches. For instance, rules for cloud architectures are the topic of works such as [30–33] that propose only partial solutions, as they either restrict the parts of the system that could be adapted or offer a limited expressiveness in the definition of the rules (e.g., no trigger condition).

Among the most powerful solutions, Lee et al. [4] present a self-adaptive framework where IoT systems are modeled as finite-state machine. However adaptations are only enabled at the device layer level and self-adaptive rules are not possible. Garlan et al. [34] present Rainbow, a framework for adapting a software system when a constraint (expressed in terms of performance, cost, or reliability) is violated. Similarly, Weyns et al. [35] propose MARTA, an architecture-based adaptation approach to automate the management of IoT systems employing runtime models. However, neither Rainbow or MARTA cover the specification of multi-layer architectures, nor rules combining them, and their rules are coarse-grained (e.g. not at the container level). Finally, Petrovic et al. [29] propose SMADA-Fog, a semantic model-driven approach to deployment and adaptation of container-based applications in Fog computing scenarios. SMADA-Fog does not allow the specification of complex adaptation rules composed of various conditions and actions. Moreover, grouping nodes and IoT devices according to their location is not possible, forbidding the possibility to apply adaptations on group of nodes belonging to a cluster or a given region.

Concerning the specification of IoT systems in underground mining domain, works such as [36–38] focus on the design or deployment of the device layer (sensors and actuators) of monitoring systems, but do not address the mine structure specification, runtime adaptations, and deployment of containerized applications. To sum up, ours is the first proposal that enables the specification, deployment and execution of multi-layer IoT architectures (device, edge, fog, and cloud) and the definition of complex rules covering all layers (and combinations of) involving multiple conditions and actions that can, potentially, engage groups of nodes in the same region or cluster of the IoT system. Moreover, our proposal can be easily extended and specialized in different domains as shown with the underground mining scenario.

8 Conclusions and Future Work

We have presented a model-based approach for the specification and runtime execution of multi-layered architectures of IoT systems and their self-adaptation rules. Our approach comprises a new DSL to model such systems, a code generator, and a runtime infrastructure, based on the MAPE-K loop, to monitor and execute the IoT system at runtime based on a variety of rules,

involving architectural adaptations and rules to address functional requirements. The full process is assisted by a set of open-source tools that have been released as part of this work. We have also validated the usability and extensibility of the DSL.

As part of our future work, we will continue to enrich the DSL based on the suggestions made by the experiment participants, including a new visual renderer of the modeled architecture to complement the current projections. We also plan to facilitate the definition of complex self-adaptive rules by predefining a set of common patterns such as *canary*, *rolling update*, and *blue-green* deployment strategies that could be directly referenced in the definition of a rule. Moreover, we are also interested to automatically discover potentially useful adaptation rules by analyzing historical log data from the IoT system (e.g., focusing on previous system crashes) with machine learning. Finally, we are creating additional extensions to the DSL. In particular, one to model Wastewater Treatment Plants as part of an ongoing European project.

References

- [1] Jiang, Y., Huang, Z., Tsang, D.H.: Challenges and solutions in fog computing orchestration. *IEEE Network* **32**(3), 122–129 (2017)
- [2] Rhayem, A., Mhiri, M.B.A., Gargouri, F.: Semantic web technologies for the internet of things: Systematic literature review. *Internet of Things* **11**, 100206 (2020)
- [3] Brambilla, M., Cabot, J., Wimmer, M.: *Model-driven Software Engineering in Practice*, 2nd Edn. Synthesis Lectures on Software Engineering. Morgan & Claypool Publishers, USA (2017)
- [4] Lee, E., Seo, Y.-D., Kim, Y.-G.: Self-adaptive framework based on mape loop for internet of things. *sensors* **19**(13), 2996 (2019)
- [5] Patel, P., Cassou, D.: Enabling high-level application development for the internet of things. *Journal of Systems and Software* **103**, 62–84 (2015)
- [6] Ciccozzi, F., Spalazzese, R.: Mde4iot: supporting the internet of things with model-driven engineering. In: *Int. Symposium on Intelligent and Distributed Computing*, pp. 67–76 (2016)
- [7] Yigitoglu, E., Mohamed, M., Liu, L., Ludwig, H.: Foggy: a framework for continuous automated IoT application deployment in fog computing. In: *IEEE Int. Conf. on AI & Mobile Services*, pp. 38–45 (2017)
- [8] Alfonso, I., Garcés, K., Castro, H., Cabot, J.: Modeling self-adaptive IoT architectures. In: *2021 ACM/IEEE Int. Conf. on Model Driven Engineering Languages and Systems Companion*, pp. 761–766 (2021)

- [9] Kephart, J.O., Chess, D.M.: The vision of autonomic computing. *Computer* **36**(1), 41–50 (2003)
- [10] Latifah, A., Supangkat, S.H., Ramelan, A.: Smart building: A literature review. In: *Int. Conf. on ICT for Smart Society (ICISS)*, pp. 1–6 (2020)
- [11] Alfonso, I., Garcés, K., Castro, H., Cabot, J.: Self-adaptive architectures in IoT systems: a systematic literature review. *Journal of Internet Services and Applications* **12**(1), 1–28 (2021)
- [12] Al-Qamash, A., Soliman, I., Abulibdeh, R., Saleh, M.: Cloud, fog, and edge computing: A software engineering perspective. In: *2018 Int. Conf. on Computer and Applications (ICCA)*, pp. 276–284 (2018). IEEE
- [13] Shi, W., Cao, J., Zhang, Q., Li, Y., Xu, L.: Edge computing: Vision and challenges. *IEEE internet of things journal* **3**(5), 637–646 (2016)
- [14] Dustdar, S., Avasalcai, C., Murturi, I.: Edge and fog computing: Vision and research challenges. In: *2019 IEEE Int. Conf. on Service-Oriented System Engineering (SOSE)*, pp. 96–9609 (2019). IEEE
- [15] Yousefpour, A., Fung, C., Nguyen, T., Kadiyala, K., Jalali, F., Niakanlahiji, A., Kong, J., Jue, J.P.: All one needs to know about fog computing and related edge computing paradigms: A complete survey. *Journal of Systems Architecture* **98**, 289–330 (2019)
- [16] Mansouri, Y., Babar, M.A.: A review of edge computing: Features and resource virtualization. *Journal of Parallel and Distributed Computing* **150**, 155–183 (2021)
- [17] Gómez, A., Iglesias-Urkia, M., Belategi, L., Mendialdua, X., Cabot, J.: Model-driven development of asynchronous message-driven architectures with asyncapi. *Software and Systems Modeling*, 1–29 (2021)
- [18] Mishra, B., Kertesz, A.: The use of mqtt in m2m and iot systems: A survey. *IEEE Access* **8**, 201071–201086 (2020)
- [19] Berger, T., Völter, M., Jensen, H.P., Dangprasert, T., Siegmund, J.: Efficiency of projectional editing: A controlled experiment. In: *Proc. of the 24th ACM SIGSOFT Int. Symposium on Foundations of Software Engineering*, pp. 763–774 (2016)
- [20] Alfonso, I., Garcés, K., Castro, H., Cabot, J.: Self-adaptive IoT DSL. <https://github.com/SOM-Research/selfadaptive-IoT-DSL> (2022)
- [21] Rubin, J., Chisnell, D.: *Handbook of Usability Testing: How to Plan, Design and Conduct Effective Tests*. John Wiley & Sons, New Jersey

(2008)

- [22] Nielsen, J., Landauer, T.K.: A mathematical model of the finding of usability problems. In: Proc. of the INTERACT'93 and CHI'93 Conf. on Human Factors in Computing Systems, pp. 206–213 (1993)
- [23] Sandobalin, J., Insfran, E., Abrahão, S.: ARGON: A model-driven infrastructure provisioning tool. In: ACM/IEEE 22nd Int. Conf. on Model Driven Engineering Languages and Systems Companion (MODELS-C), pp. 738–742 (2019)
- [24] Sledziewski, K., Bordbar, B., Anane, R.: A DSL-based approach to software development and deployment on cloud. In: 24th IEEE Int. Conf. on Advanced Information Networking and Applications, pp. 414–421 (2010)
- [25] Bergmayr, A., Breitenbücher, U., Kopp, O., Wimmer, M., Kappel, G., Leymann, F.: From architecture modeling to application provisioning for the cloud by combining uml and toscala. In: 6th Int. Conf. on Cloud Computing and Services Science, pp. 97–108 (2016)
- [26] Gomes, T., Lopes, P., Alves, J., Mestre, P., Cabral, J., Monteiro, J.L., Tavares, A.: A modeling domain-specific language for IoT-enabled operating systems. In: IECON 2017-43rd Annual Conf. of the IEEE Industrial Electronics Society, pp. 3945–3950 (2017)
- [27] Eterovic, T., Kaljic, E., Donko, D., Salihbegovic, A., Ribic, S.: An internet of things visual domain specific modeling language based on UML. In: 2015 XXV Int. Conf. on Information, Communication and Automation Technologies (ICAT), pp. 1–5 (2015)
- [28] Barriga, J.A., Clemente, P.J., Sosa-Sánchez, E., Prieto, Á.E.: Simulateiot: Domain specific language to design, code generation and execute iot simulation environments. *IEEE Access* **9**, 92531–92552 (2021)
- [29] Petrovic, N., Tomic, M.: Smada-fog: Semantic model driven approach to deployment and adaptivity in fog computing. *Simulation Modelling Practice and Theory* **101**, 102033 (2020)
- [30] Ferry, N., Chauvel, F., Song, H., Rossini, A., Lushpenko, M., Solberg, A.: Cloudmf: Model-driven management of multi-cloud applications. *ACM Transactions on Internet Technology (TOIT)* **18**(2), 1–24 (2018)
- [31] Chen, W., Liang, C., Wan, Y., Gao, C., Wu, G., Wei, J., Huang, T.: MORE: A model-driven operation service for cloud-based it systems. In: IEEE Int. Conf. on Services Computing, pp. 633–640 (2016)
- [32] Erbel, J., Korte, F., Grabowski, J.: Comparison and runtime adaptation

- of cloud application topologies based on OCCI. In: The 8th Int. Conf. on Cloud Computing and Services Science, pp. 517–525 (2018)
- [33] Cámara, J., Muccini, H., Vaidhyanathan, K.: Quantitative verification-aided machine learning: A tandem approach for architecting self-adaptive IoT systems. In: 2020 IEEE Int. Conf. on Software Architecture (ICSA), pp. 11–22 (2020)
 - [34] Garlan, D., Schmerl, B., Cheng, S.-W.: Software architecture-based self-adaptation. In: Autonomic Computing and Networking, pp. 31–55 (2009)
 - [35] Weyns, D., Iftikhar, M.U., Hughes, D., Matthys, N.: Applying architecture-based adaptation to automate the management of internet-of-things. In: European Conf. on Software Architecture, pp. 49–67 (2018)
 - [36] Porselvi, T., Ganesh, S., Janaki, B., Priyadarshini, K., *et al.*: IoT based coal mine safety and health monitoring system using lorawan. In: 2021 3rd Int. Conf. on Signal Processing and Communication, pp. 49–53 (2021)
 - [37] Mishra, P., Kumar, S., Kumar, M., Kumar, J., *et al.*: IoT based multimode sensing platform for underground coal mines. *Wireless Personal Communications* **108**(2), 1227–1242 (2019)
 - [38] Alfonso, I., Gómez, C., Garcés, K., Chavarriaga, J.: Lifetime optimization of wireless sensor networks for gas monitoring in underground coal mining. In: 7th Int. Conf. on Computers Comms. and Control, pp. 224–230 (2018)

A DSL Usability Validation

In this appendix, we present complementary information on the DSL usability and expressiveness validation experiments. For Experiment 1, we discuss the expertise of the participants, while for Experiment 2 we present the design of the experiment and the results obtained, including the suggestions and opinions of the participants.

A.1 Experiment 1: DSL Usability Validation - Mining Concepts

Figure 10 presents the level of general mining knowledge (very low, low, medium, high, and very high) of the eight participants. All of them are aware of the terminology used in the design and structure of underground coal mines. Only two participants were not familiar with cyber-physical or IoT systems for mining.

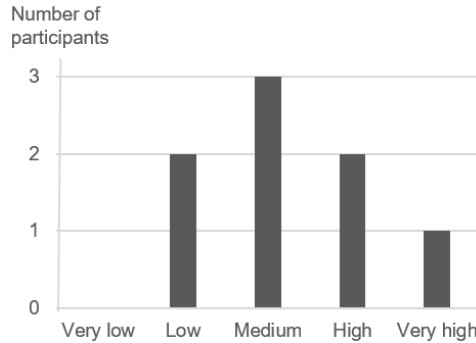


Fig. 10 Participants' mining expertise

A.2 Experiment 2: DSL Usability Validation - Architectural Concepts

The second experiment aimed to validate the expressiveness and easy of use of concepts more focused on multi-level cloud architecture modeling: edge, fog, and cloud nodes, container-based applications, and architecture adaptation rules. Five computer science researchers accepted our invitation to participate in this experiment. A pre-questionnaire and an exercise divided into two sessions (Sessions 1 and 2) was conducted.

A.2.1 Experiment design and setup

The experiment consisted of an asynchronous screening test (pre-questionnaire) to assess subjects' prior knowledge and suitability for participation, and a synchronous exercise (virtual meeting) with two parts (Sessions

1 and 2). The materials and exercises provided to the participants, the questionnaires and the anonymized answers can be found in the repository of our DSL extended to the mining industry domain²³.

- Pre-questionnaire (10 min): the questionnaire Q0 (screening test) was completed by the participants to ensure that they had a basic level of knowledge of IoT systems, containerization technologies, and modeling tools.
- Session 1 (50 min): we have introduced a 20 minutes presentation with the basic concepts of IoT system architectures (layers, nodes, container-based applications) and modeling examples to describe the architecture using the DSL. Then the participants performed a modeling exercise of an IoT system architecture with five edge nodes, two fog nodes, one cloud node, and several software containers. Finally, the questionnaire Q1 was filled out about the expressiveness and ease of use of the DSL for modeling the system architecture.
- Session 2 (40 min): We have presented the basic concepts and examples for specifying system architecture adaptation rules. Then, participants performed a modeling exercise of five architecture adaptation rules involving infrastructure metrics (such as CPU consumption, RAM, and availability) and architecture adaptations such as application scaling or container offloading. Finally, the questionnaire Q2 was completed to gather information about the expressiveness and ease of use perceived by the participants.

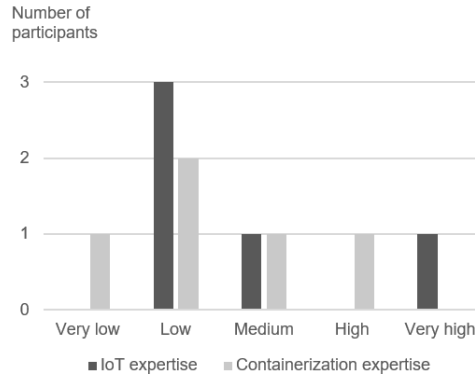
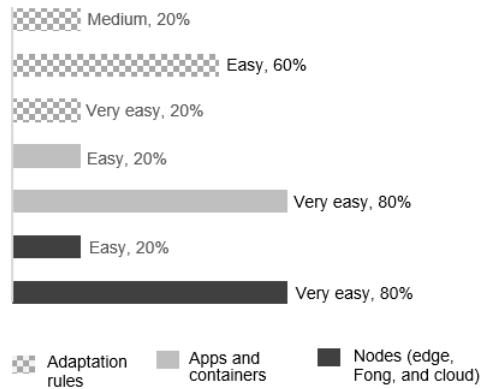
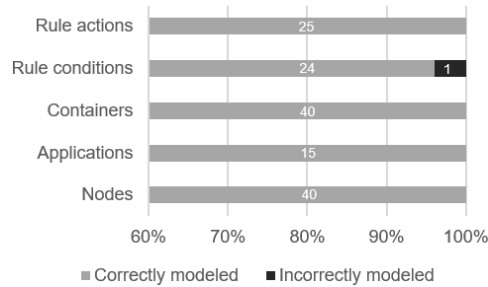
The experiment was conducted in Spanish on three different dates in 2022. The PhD student of this thesis conducted the virtual meetings and ensured that all were equally well executed.

A.2.2 Results

Figure 11 shows the level of knowledge reported by the participants about IoT systems (architecture, deployment, and operation) and containerization as a virtualization technology. Although most participants reported a low level knowledge, they are familiar with monitoring QoS metrics (such as latency, availability, bandwidth, CPU consumption) and architecture adaptations such as auto-scaling and offloading.

According to the information collected from the questionnaires, most participants have reported that it was very easy or easy to model the system architecture (nodes, applications and containers) and its adaptation rules (see Figure ref). Furthermore, the results presented in Figure ref (errors in the models built by the participants) demonstrate the ease of use, even for non-expert users in the IoT domain. The only mistake made by a participant in specifying the condition of an adaptation rule was a wrong selection of the *targetNode* to be checked.

²³<https://github.com/SOM-Research/IoT-Mining-DSL>

**Fig. 11** IoT and containerization expertise of participants**Fig. 12** DSL ease of use (experiment 2)**Fig. 13** Percentage and number of right and wrong answers (experiment 2)

The suggestions and opinions of the participants about including new features or improvements to the DSL are as follows:

- Some suggestions about typo errors and minor interface improvements (editors) were reported and have already been addressed.
- Although the DSL provides textual and tabular notation for modeling the architecture nodes, including graphical notation (such as a deployment diagram) could be useful to easily follow the hierarchy of the architecture nodes.
- There may be applications that require more than one port to be exposed. However, the DSL does not allow more than one port to be associated with each application. The suggestion is to enable the specification of multiple ports for a single application.

B Evaluation of System Self-Adaptations

To evaluate the self-adaptation capability of our approach, we conducted three empirical evaluations, one for each type of adaptation (scaling, offloading, and redeployment). For each adaptation assessment we have designed a simple scenario in which an IoT system faces an event that forces adaptations. **The goal of this experiments** is to compare the availability and performance of a non-adaptive IoT system with that of a self-adaptive IoT system that is modeled and managed using our approach. To do so, we have collected and analyzed metrics such as CPU consumption, node availability, and data processing time.

B.1 Experiment Design and Setup

To test the three architectural adaptations, we have designed a test scenario with the IoT system shown in Figure 14. The system architecture consists of four temperature sensors, two edge nodes (t2.micro AWS instances²⁴), one fog node (t2.medium AWS instance), and three applications (*broker-app*, *realtime-app*, and *predictive-app*) executed by four software containers (C1, C2, C3, and C4).

- *broker-app*: MQTT broker that manages messages published by sensor devices. We used Eclipse Mosquitto²⁵ as message broker because it is lightweight, easy to configure, and is suitable for running at the edge layer. This broker is deployed on the *edge-2* node and executed by the C1 container.
- *realtime-app*: application subscribed to the MQTT broker to consume the data, coming from the sensors, and perform real-time data analysis. For each sensor data received on the broker topics, this application creates a thread or subprocess that performs a series of operations to intentionally generate workload on the node. After processing each sensor data, the result is published in another broker topic.
- *predictive-app*: this application simulates the execution of a predictive algorithm to forecast possible temperature emergencies. The algorithm (subscribed to the broker's topics) receives data from sensors and performs mathematical routines using the NumPy²⁶ package.

Additionally, we have developed a Python script which publishes random values on topics of the MQTT broker to simulate the four temperature sensors. During the experiment, the sampling rate of the sensors is increased incrementally to perturb the system and induce self-adaptation.

Figure 14 does not show how containers C2, C3, and C4 are deployed on the nodes, because the use of these containers will depend on the type of

²⁴<https://aws.amazon.com/es/ec2/instance-types/t2/>

²⁵<https://mosquitto.org/>

²⁶<https://numpy.org/>

adaptation to be tested. Section B.2 shows the protocol of the experiments including the deployment and adaptation of these containers.

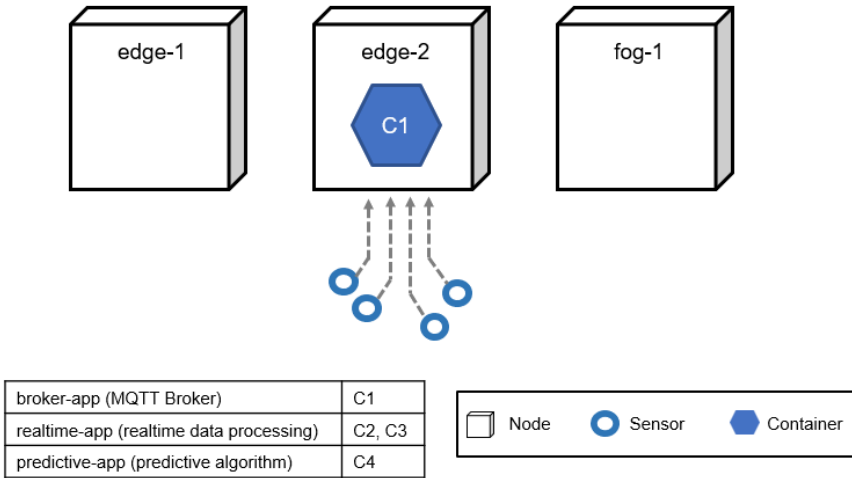


Fig. 14 General test scenario for adaptations

B.2 Experiment Protocol

For each type of architectural adaptation we performed an experiment that generally follows the same protocol consisting of the following steps:

1. Model the IoT system (using our DSL) including the adaptation rule to be tested.
2. Run the code generator using the model built in the first step.
3. Deploy the IoT applications and execute our runtime framework using the YAML manifests built by the code generator.
4. Generate disturbances or dynamic events and monitor availability and performance of the system when: (a) the system has no self-adaptation capabilities, and (b) the system self-adapts using our framework.

The variable we manipulate in these experiments (**independent variable**) is the sampling frequency of the sensors in order to generate node overhead, while the variables we monitor (**dependent variables**) are the availability and performance of the nodes. Although the protocol of the three experiments are similar, some aspects change depending on the type of adaptation (scaling, offloading, redeploying) to be tested.

B.2.1 Scaling an application

The experiment scenario to test *Scaling* adaptation consists of two steps as shown in Figure 15.

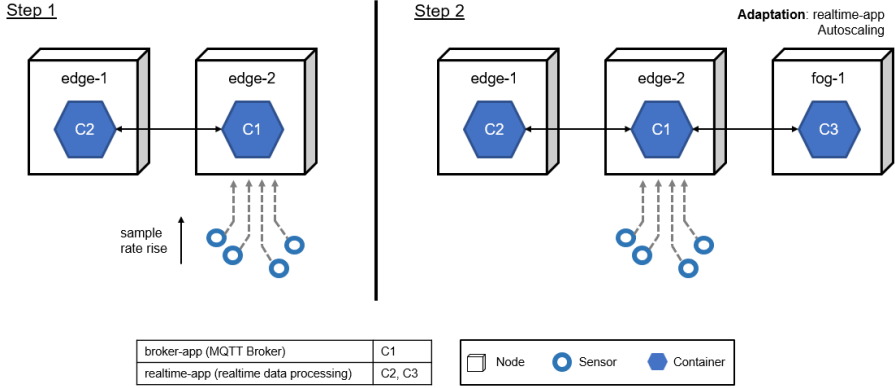


Fig. 15 Scaling adaptation test scenario

In step 1, we gradually increase the sampling or monitoring frequency of the sensors to overload the *edge-1* node by increasing the amount of data to be processed by the *C2* container. Initially, we simulate sending 5 data per second to the MQTT broker for two minutes. Then we increase to 12 data per second for the next two minutes. Finally we increase to 30 data per second.

In step 2, after overloading the *edge-1* node, the realtime-app application is scaled. The *Adaptation Engine* of our framework deploys the *C3* container on the *fog-1* node. Then, the data coming from the sensors are distributed for analysis between the *C2* and *C3* containers. This distribution of messages among subscribers is achieved by a balancing strategy known as MQTT shared subscription [16]. In a shared subscription, all clients sharing the same subscription receive messages alternately, i.e., each message will only be sent to one of the subscribed clients.

Figure 16 shows the adaptation rule that we have specified using the DSL to test the *Scalability* adaptation. This rule states that if the CPU usage of the *edge-1* node is greater than 80% for 30 seconds, then scale an instance of the *realtime-app* application on the *fog-1* node. For this adaptation rule, we have chosen to check the CPU usage of the node as it is a metric that reflects the work overhead of the node.

Scaling App

```
Condition: ( cpu[edge-1] ) > ( 80 % )
Period: 30 s
Actions:
  * Scaling -> Application: realtime-app
                Instances: 1
                Target node(s): fog-1
                Target region(s): << ... >>
                Target cluster: << ... >>
```

Fig. 16 Scaling adaptation rule

B.2.2 Offloading a container

The experiment scenario to test the *Offloading* adaptation consists of two steps as shown in Figure 17.

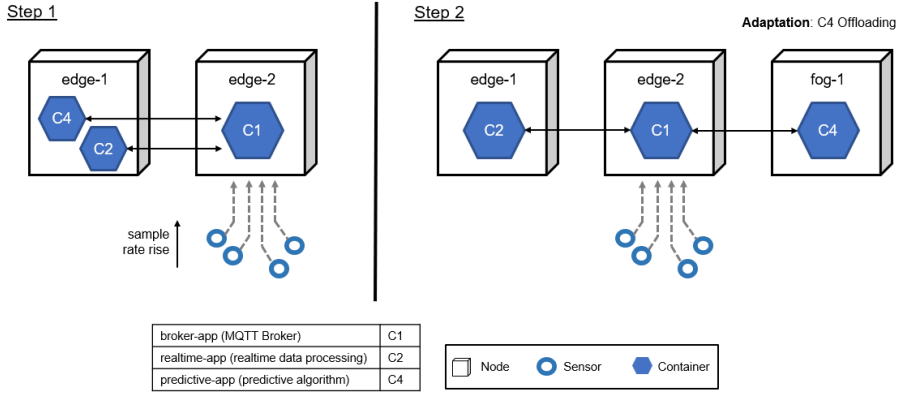


Fig. 17 *Offloading* adaptation test scenario

Similar to our previous experiment, in step 1 the sampling frequency of the sensors is gradually increased (5, 12 and 20 data per second) until an overload is generated in the node *edge-1* due to the increase of sensor data processed by the *C2* container. This node (*edge-1*) hosts the *C2* and *C4* containers that run the *realtime-app* and *predictive-app* applications. Then, in step 2, the system offloads the *C4* container to the *fog-1* node freeing resources on the *edge-1* node.

The adaptation rule modeled is shown in Figure 18: if the CPU usage of node *edge-1* exceeds 80% for 30 seconds, then the *C4* container is offloaded to node *fog-1*.

Offloading C4

```

Condition: ( cpu[edge-1] ) > ( 80 % )
Period: 30 s
Actions:
  * Offloading -> Container: C4
    Target node(s): fog-1
    Target region(s): << ... >>
    Target cluster: << ... >>

```

Fig. 18 *Offloading* adaptation rule

B.2.3 Redeploying a container

The scenario for testing the *Redeployment* adaptation is the same as shown in Figure 14. First we force a bug in the C1 container by logging into the pod using the command line tool and stopping some system processes. Then, our runtime framework, which constantly monitors the state of containers, detects container unavailability and redeploys it using the *Adaptation Engine*.

The adaptation rule modeled for testing the *Redeployment* of a container is shown in Figure 19. If the container *C1* is detected to be unavailable for more than 20 seconds, then it is redeployed.

```

Redeploying C1
Condition: ( unavailability[C1] )
Period: 20 s
Actions:
    * Redeployment -> Container: C1

```

Fig. 19 *Redeployment* adaptation rule

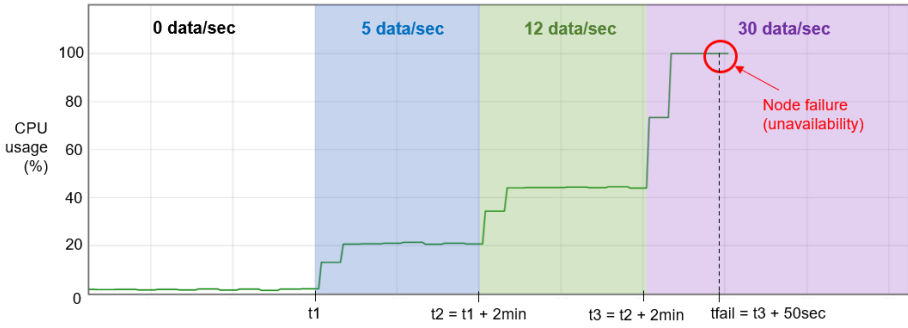
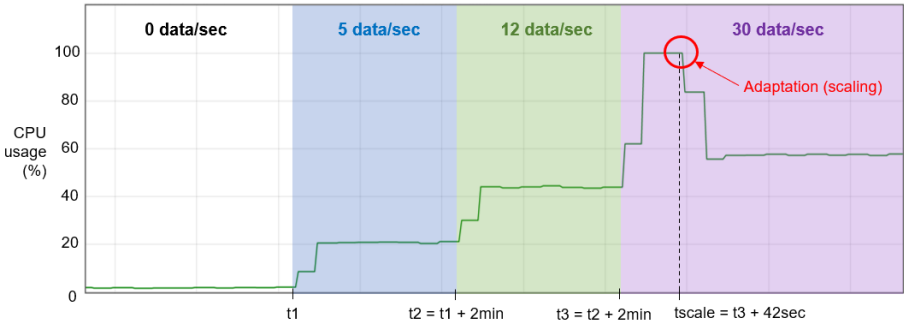
B.3 Results

In the test scenario for each type of adaptation, the system was monitored in two cases: (1) without implementing adaptations, and (2) self-adapting the system according to the configured adaptation rules. The results for each type of adaptation are compared below.

B.3.1 Scaling an application

Figure 20 presents the CPU usage of the *edge-1* node by increasing the sampling frequency of the sensors. The colored shaded areas represent different sampling frequencies of the sensors. The blue shading indicates that the sensors publish data to the broker at a frequency of 5 data/sec, the green shading 12 data/sec, and the purple shading 30 data/sec. For both cases (non-adaptive and self-adaptive), it was evidenced how the CPU consumption of the node increased when the amount of data to be processed increased too. However, when the CPU usage grew to 100%, the *edge-1* node failed at *tfail* time (Figure 20(a)) for the case of not using adaptations, while implementing the adaptation rule the system auto-scaled the *realtime-app* application (at *tscale* time), the workload was reduced for the *edge-1* node (20(b)), preventing it from failing.

Similarly, Figure 21 shows the time spent by the C2 container to process the data published in the broker by the sensors. For a non-adaptive system (Figure 21(a)) the processing time for some data was reached to grow up to 13.5 sec until the node failed due to work overload. On the other hand, the self-adaptive system (Figure 21(b)) reached processing times of 8.8 sec, then the system auto-scaled the *realtime-app* application at *tscale* time and the data processing time dropped back below 1 sec.

(a) *edge-1* node CPU usage (non-adaptive system)(b) *edge-1* node CPU usage (self-adaptive system; scaling the *realtime-app*) application**Fig. 20** *edge-1* node CPU usage; scaling adaptation

B.3.2 Offloading a container

The CPU consumption of the *edge-1* node is shown in Figure 22. As in the results of the *Scaling* adaptation fitting, the colored shades in the figure represent different data sending frequencies from the sensors. Note that there is a constant CPU usage (43% approx.) before increasing the sampling frequency of the sensors. This CPU usage is caused by *C4* container that simulates the predictive algorithm. As the sampling frequency increased, the CPU consumption of the node also increased. For the non-adaptive system (Figure 22(a)) the node overloaded (CPU usage reached 100%) and failed 26 seconds (t_{fail}) after increasing the sampling rate from 12 to 20 data per second. In the case of the self-adaptive system, the CPU consumption of the node did not reach 100% due to the adaptation. The *C4* container was offloaded to the *fog-1* node at $t_{offload}$ time reducing the workload on the *edge-1* node, preventing it from failing.

Figure 23 shows the processing time of the *C2* container data. This processing time increased considerably when the node used 100% of CPU as is the case of the non-adaptive system (Figure 23(b)), in which the processing time of some data reached 17 seconds before the node failed. On the other hand,

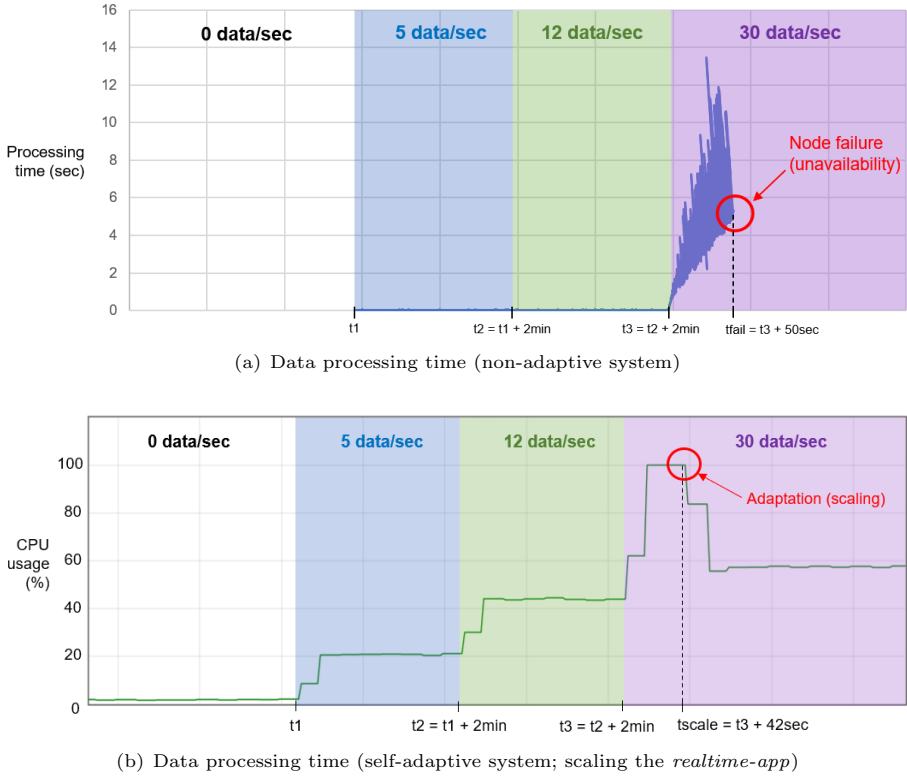


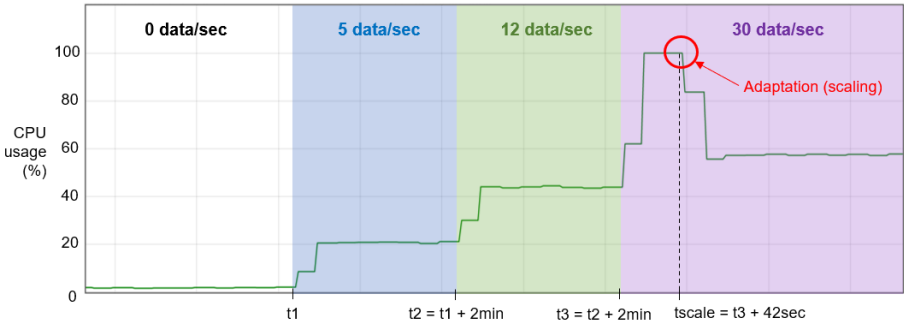
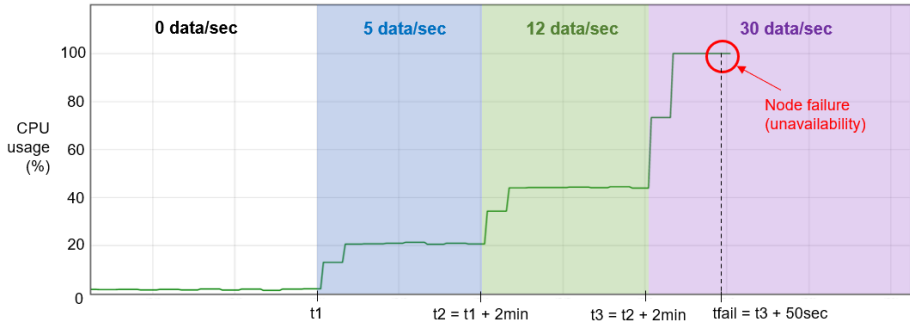
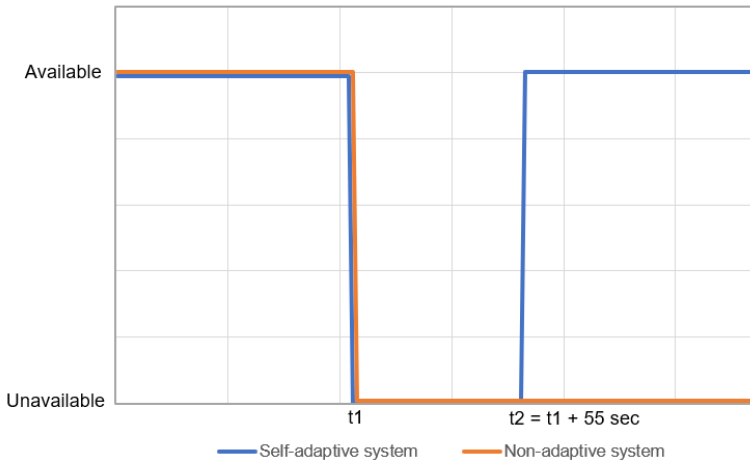
Fig. 21 Processing time data of *C2* container; scaling adaptation

the self-adaptive system experience processing times of less than 0.3 seconds. This behavior because the *edge-1* node never reached high CPU consumption.

B.3.3 Redeploying a container

For this Redeployment test, the dependent variable is the availability of the container to be adapted (i.e. to be redeployed). Therefore, we present and analyze the results about the availability of the container.

Figure 24 shows the state (available or unavailable) of the *C4* container for both cases: non-adaptive and self-adaptive systems. In the case of the non-adaptive system, the container is unavailable once its failure has been induced at time $t1$. On the contrary case, the self-adaptive system detects that the container is unavailable for 20 seconds and starts the redeployment process. It took approximately 35 seconds to remove the *C4* container and redeploy it. After this procedure, the container changed its status to available again.

**Fig. 22** *edge-1* node CPU usage; offloading adaptation**Fig. 24** Availability of the *C4* container

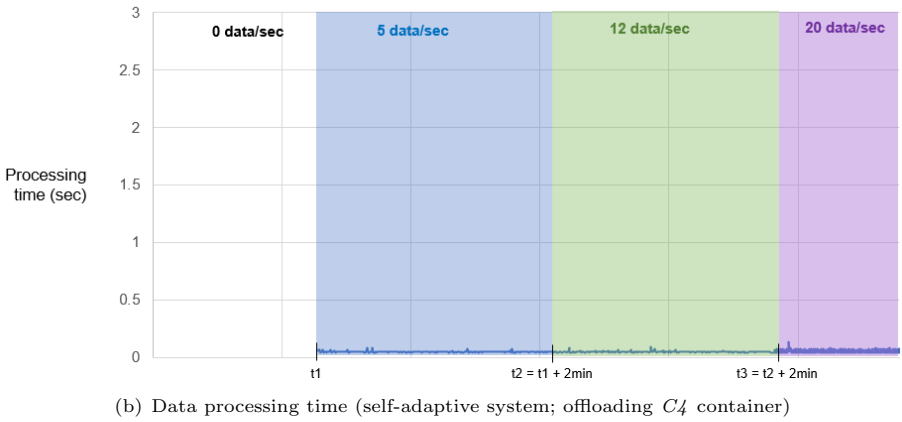
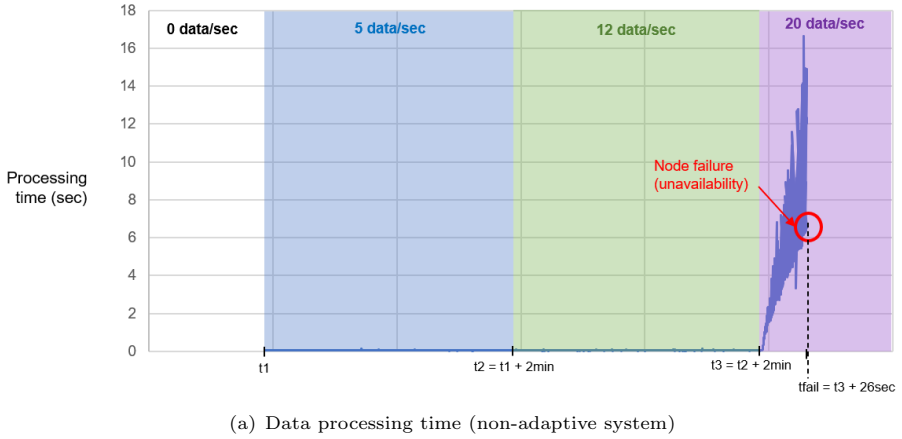


Fig. 23 Processing time data of C_2 container; offloading adaptation

B.4 Threats to Validity

The threats identified in this experiment and how we addressed them are presented below.

Random irrelevancies in the setting: some factors outside the experiment (such as network instability or unexpected node failures) could disturb the outcome. In this experiment, we tried to guarantee the stability of the infrastructure using AWS cloud services, which guarantee high availability. Additionally, to avoid disturbances in the delivery of the data sent by sensors, we ran the scripts (simulating the sensors) on an EC2 instance of AWS deployed in the same virtual private cloud as the nodes. This way we guarantee that the data generated in the device layer will be published in the broker on a regular basis and with low latency.

Measurements of dependent variables should be reliable: to ensure the reliability of the measurement of dependent variables (e.g., latency and

availability), we have run each experiment at least three times and obtained very similar results. To collect these variables data, we used the monitors and exporters deployed by the framework and consulted the information in the Prometheus time series database.

Mono-operation bias: the study should include the analysis of more than one dependent variable. In our experiments, we analyzed various QoS metrics and infrastructure of nodes and containers. For example, we collected and displayed CPU utilization, availability, and data processing latency. Additionally, for the *Redeploying* a container adaptation experiment, in addition to analyzing the availability metric, we also capture the unavailability time of the container while it is redeployed.

Size of the test scenario: one of the threats is related to the size of the IoT system to be modeled and tested. Since the objective of this validation was to test the architectural adaptations individually, we proposed a small scenario composed of an IoT system with two edge nodes and one fog node. This scenario was sufficient to model an adaptation rule that allowed testing each adaptation. Nevertheless, we have planned a large scenario (as presented in Section C) to validate the scalability of our approach and the execution of concurrent adaptations.

C Evaluation of Framework Scalability

To evaluate the ability of our framework to address the growth of concurrent adaptations on an IoT system, we have conducted two experiments: the first one that triggers the firing of simultaneous adaptation rules composed of a single action, and the second one that triggers the firing of simultaneous adaptation rules composed of a group of actions. **The goal of this experiments** is to identify scalability limitations and boundaries to perform concurrent adaptations of our MAPE-K based framework to adapt the IoT system at runtime. The design, protocol, and results of the experiment are presented below.

C.1 Experiment Design and Setup

To test the scalability of our framework, we have designed a test scenario emulating an IoT environmental monitoring system in three underground coal mines (Figure 25). For simplicity, we assume that the three mines have the same structure (tunnels, work fronts, etc.) and the same monitoring system (nodes and applications). Each mine has ten work fronts²⁷ constantly monitored to ensure the safety of the workers. The IoT system architecture is composed as follows.

- The **device layer** is composed of several types of sensors deployed at different work fronts. Each work front contains sensors to monitor methane (CH₄), carbon dioxide (CO₂), carbon monoxide (CO), Hydrogen sulfide (H₂S), Sulfur dioxide (SO₂), nitric oxide (NO), nitrogen dioxide (NO₂), temperature, and air velocity. The information collected by the sensors is sent to a messaging broker (deployed on *edge-1* for the *Mine 1*).
- The **edge and fog layer** nodes run different applications to detect emergencies, control actuators, store information locally and aggregate information to be sent to the cloud nodes.
- The **cloud layer** nodes run a web application to query historical data about and reports on the environmental status of the three mines. A database is also deployed on one of the cloud nodes to store aggregated data.

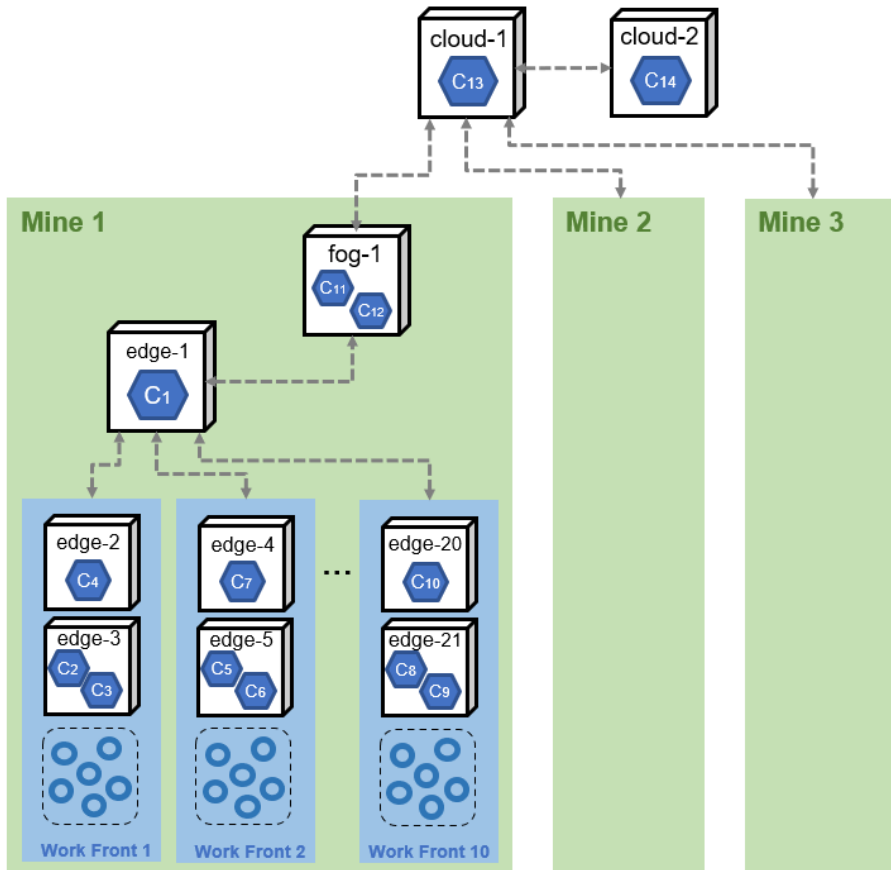
To set up the test environment, we provisioned EC2 instances from AWS. Instances t2.micro (1 vCPU and 1 GB of memory) for edge nodes, instances t2.small (1 vCPU and 2 GB of memory) for fog nodes, and instances t2.medium (2 vCPU and 4 GB of memory) for cloud nodes. The collection and sending of data from the sensors was simulated using a script written in Python language.

The containerized applications deployed on the nodes include: an MQTT broker that receives and distributes all sensor data; *stel-app* and *twa-app* check that the values of the monitored gases do not exceed their allowable STEL and TWA value; *temp-app* checks that the temperature at the different work fronts does not exceed the allowable limit value (depending on wind speed); *UI-app* is a user interface for real-time querying of sensor data; *local-database*

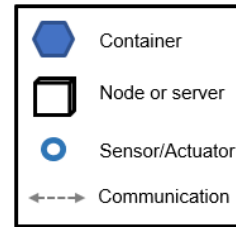
²⁷A large underground coal mine in Colombia could have around ten active work fronts, either mining, advancement, or development.

stores the data locally before being aggregated and sent to the cloud; finally, *web-app* and *cloud-database* enable to store and query the aggregated data in the cloud.

This IoT scenario for underground coal mining is intended to be as close as possible to a real implementation following the rules established in the Colombian mining regulations. For example, the STEL and TWA values are suggested by this decree. However, in this empirical validation, we have developed applications that consume the broker messages and perform some kind of analysis, but do not calculate and check the actual STEL and TWA limit values. This is because the objective of these applications is to generate workload on the nodes to test the scalability limitations of the framework.



Application	Container
broker (MQTT Broker)	C1
*stel-app (realtime gas data analysis)	C2, C5, C8
**twa-app (gas limit value 8h)	C3, C6, C9
temp-app (temperature analysis)	C4, C7, C10
UI-app (user interface)	C11
local-database	C12
web-app	C13
cloud-database	C14



* STEL value is the permissible limit value for a short exposure time (max. 15 min.)

** TWA value is the permissible limit value for an average time of 8 hours

Fig. 25 Large mining IoT system to be modeled

C.1.1 Experiment 1

In Experiment 1, we have tested the activation and execution of simultaneous adaptation rules composed of a single action. We have defined and triggered an adaptation rule for 1, 5, 10, 20, and 30 work fronts (five independent tests).

Figure 26 shows the adaptation rule for *Work Front 1* (a similar rule was specified for each work front): if the CPU consumption of node *edge-3* exceeds 80% for 60 seconds, then offload the container *c3* to node *edge-2*. In this experiment we have chosen the offloading action, which implies more effort for the *Adaptation Engine*, since it involves the removal and creation of a container on a different node.

Work Front 1 Rule

```

Condition: ( cpu[edge-3] ) > ( 80 % )
Period: 60 s
Actions:
  * Offloading -> Container: c3
                    Target node(s): edge-2
                    Target region(s): << ... >>

```

Fig. 26 Adaptation rule for *Work front 1* - single action

C.1.2 Experiment 2

In Experiment 2, we have defined adaptation rules involving several actions. Similar to Experiment 1, we have defined rules for 1, 5, 10 and 20 work fronts (4 independent tests). Figure 27 shows the adaptation rule for *Work Front 1* (for the other work fronts, the rules are similar), whose list of actions includes one offload, three scaling, and two redeployment. Note that each scaling action is intended to deploy three instances of the application to any node in the mine. This is to detect problems with the execution of concurrent adaptations and limitations in container allocation.

```

Work Front 1
Condition: ( cpu[edge-3] ) > ( 80 % )
Period: 60 s
Actions:
☒ all actions
  * Offloading -> Container: c2
                    Target node(s): edge-2
                    Target region(s): << ... >>
  * Scaling -> Application: stel-app
                    Instances: 3
                    Target node(s): << ... >>
                    Target region(s): mine1
  * Scaling -> Application: twa-app
                    Instances: 3
                    Target node(s): << ... >>
                    Target region(s): mine1
  * Scaling -> Application: temp-app
                    Instances: 2
                    Target node(s): << ... >>
                    Target region(s): mine1
  * Redeployment -> Container: c11
  * Redeployment -> Container: c4

```

Fig. 27 Adaptation rule for *Work front 1* - multiple actions

C.2 Experiment Protocol

Both Experiment 1 and Experiment 2 follow the same protocol, consisting of the following steps.

1. Model the IoT system (using our DSL) including the adaptation rules to be tested.
2. Run the code generator using the model built in the first step.
3. Deploy the IoT applications and execute our runtime framework using the YAML manifests built by the code generator.
4. Execute the Python script that simulates the generation of sensor data and publishes the messages to the broker. In this way, the necessary workload is generated on the nodes for the adaptation rules to be fired.

The independent variable in both experiments is the frequency of data generation. We set the necessary data frequency (90 samples per minute for each sensor) to trigger the adaptation rules. As for the dependent variables, in Experiment 1 we focused on monitoring the time spent by the system to detect the event, to generate the adaptation plan, and to adapt the system. In Experiment 2, in addition to monitoring the time spent on adaptation, we also focused on analyzing the number of errors performing adaptations and the reasons for them.

C.3 Results and Analysis

C.3.1 Experiment 1

Figure 28 shows the results of the tests performed in this experiment. The information in the table includes the number of adaptation rules configured in the test; the number of errors or failed adaptations; the detection delay refers to the time it takes the system (Prometheus Alerting rules) from the detection of the first rule, to the last one (e.g., for test # 2, the system takes 10,30 seconds from the detection of the event of rule 1 to the detection of the event of rule 5); the time it takes Prometheus Alert Manager to generate the adaptation plan and send it to the Adaptation Engine; and finally, the time it takes the Adaptation Engine to perform the Offloading adaptation, which involves the creation of a new container and the deletion of the old one.

The time spent in the monitoring stage to collect QoS and infrastructure metrics has not been monitored because this is a configurable fixed value for Prometheus. For these experiments, we have set the Prometheus monitoring frequency equal to 4 times every minute (i.e., monitoring every 15 seconds), and the rule evaluation frequency equal to 6 times per minute (i.e., evaluation every 10 seconds). These values were adequate to not generate significant workload on the edge nodes (EC2 t2.micro instances with limited resources).

Test #	Number of rules	Errors	Event detection delay (s)	Adaptation plan design time (s)	Average adaptation time (s)		
					Container creation	Container deletion	Total time
1	1	0	--	1.10	2.06	31.34	33.40
2	5	0	10.30	1.07	2.09	31.32	33.41
3	10	0	12.59	1.12	1.98	31.46	33.44
4	20	0	14.26	1.17	2.19	31.44	33.62
5	30	0	9.96	1.15	2.35	31.40	33.80

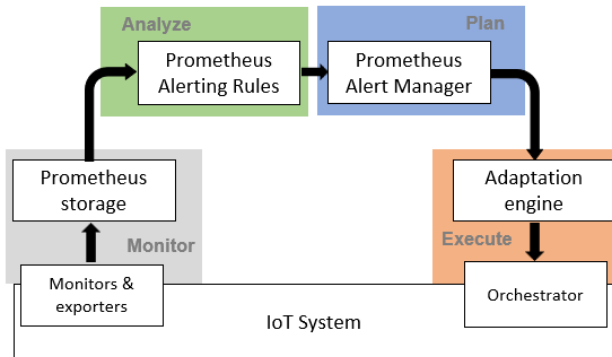


Fig. 28 Experiment 1 results

Findings from the results of this experiment are presented below.

- Ideally the event detection delay (column 4 in Table of Figure 28) should be equal to zero, i.e., all events should be detected at the same time since the increase in CPU consumption was caused at the same time in all nodes. However, there are delays between 10 and 15 seconds approximately, due to the parameters configured in Prometheus (monitoring frequency and rule evaluation frequency). If the monitoring and evaluation frequencies are increased, the event detection delays could be reduced. However, increasing these frequencies would produce significant workload on resource-poor nodes.
- In all cases (even configuring 30 adaptation rules), all actions (offloading) were performed successfully. Approximately one second is required for Prometheus Alert Manager to process an alert, generate the adaptation plan, and send it to the Adaptation Engine. The adaptation time depends on the type of action: the Adaptation Engine, via the K3S orchestrator, takes approximately 2 seconds to create a pod (which hosts a container) and 31 seconds to delete a pod. In this experiment, the MAPE-K components did not fail. However, in the next experiment (Experiment 2) we subjected the framework to more exhaustive tests to detect limitations.
- The average time taken by the adaptation engine to perform a container offload is about 33 seconds, with the removal of the container being the most time consuming task (about 31 seconds). This time is due to the grace period (default 30 seconds) that K3S uses to perform the termination of a pod. When K3S receives the command or API call to terminate a pod, it immediately changes its status to "Terminating" and stops sending traffic to the pod. When the grace period expires, all processes within the pod are killed and the pod is removed. Although our DSL does not currently support grace period configuration, we plan to include the specification of this parameter to ensure safe termination of containers in adaptations that require it (such as offloading or redeployment).

C.3.2 Experiment 2

In Experiment 2, we set up adaptation rules composed of several actions (as the rule shown in Figure 27). The results obtained are presented in Figure 29, including the number of test rules and actions, the number of failed or unsuccessful actions, the number of nodes that failed, and the average time taken by the Adaptation Engine to perform the successful actions.

Findings from the results of this experiment are presented below.

- For tests 1 and 2 all actions were performed successfully. However, tests 3 and 4 presented failed actions, mainly Scaling type actions (A2, A3, and A4). These scaling actions were not completed, because there were no more resources available on any of the mine nodes to deploy the new container instances. Even some edge nodes (5 for test 3 and 21 for test 4) failed due to work overload causing that some of the A6 actions were also not completed successfully. These results demonstrate that the successful implementation

Test #	Number of rules	Failed actions	Failed nodes	Average time of completed actions (s)					
				A1	A2	A3	A4	A5	A6
1	1 rule 6 actions	0	0	33.46	6.3	6.34	2.17	33.39	32.21
2	5 rules 30 actions	0	0	34.38	6.86	6.32	4.24	32.38	33.22
3	10 rules 60 actions	2 failed A2 actions 7 failed A3 actions 10 failed A4 actions 2 failed A6 actions	5	34.22	6.55	6.45	4.11	32.31	32.34
4	20 rules 120 actions	6 failed A2 actions 14 failed A3 actions 19 failed A4 actions 7 failed A6 actions	21	34.32	6.86	6.92	4.31	32.35	33.31

Actions		
A1. Offload container	A2. Scaling (3 instances of stel-app)	A3. Scaling (3 instances of twa-app)
A4. Scaling (2 instances of temp-app)	A5. Redeploy container	A6. Redeploy container

Fig. 29 Experiment 2 results

of the adaptations strongly relies on the availability of resources of the target nodes of the actions. In this sense, one of the improvements for our DSL could be to generate warnings to the user when insufficient resources are detected to perform the modeled adaptation rules. In this way we could prevent the implementation of infeasible rules that could fail due to lack of resources.

- The nodes that failed during tests 3 and 4 showed high CPU consumption due to the number of containers assigned to them. Whenever a new pod is deployed on a cluster of nodes (e.g., on one of the edge nodes in mine1), the Kubernetes Scheduler²⁸ becomes responsible for finding the best node for that pod to run on. Although the Scheduler checks the node resources, it does not analyze the real-time consumption of CPU and Ram memory. Therefore, for Scaling actions in tests 3 and 4, the Scheduler assigned containers to nodes (without checking their current state) causing them to fail. The design and implementation of a Scheduler that analyzes real-time metrics (such as CPU consumption) could avoid this kind of errors.
- The types of actions that require more time to be performed are Offloading and Redeployment. This is because these actions involve the removal of a pod, a task that takes about 31 seconds due to the default grace period set by the K3S orchestrator. On the other hand, the average time it takes to perform the Scalin action depends on the number of instances to be deployed. The Adaptation Engine takes about six seconds to scale three pods or containers, while it takes about four seconds to scale two pods or containers.

²⁸<https://kubernetes.io/docs/concepts/scheduling-eviction/kube-scheduler/>

C.4 Threats to Validity

The threat *random irrelevances in the setting* was addressed in the same way as we discussed in Section B.4. Other threats identified in this experiment and how we addressed them are presented below.

Measurements of dependent variables should be reliable: to ensure the reliability of the measurement of the dependent variables (e.g., time consumed adapting the system), we performed each experiment at least three times and obtained very similar results. To obtain these metrics, we generated and reviewed log files that record the time and result of each of the tasks performed by the framework components. For example, a log file records the time at which the Adaptation Engine receives the adaptation plan, the time at which each action finishes (including the K3S API command responses), and the result.

Mono-operation bias: To avoid this threat, we have planned two experiments involving several tests. Each experiment contains different adaptation rules to analyze constraints on the performance of concurrent adaptations. We increased the number of configured rules and collected more than one dependent variable to analyze the system behavior.

Size of the test scenario: The number of nodes (edge, fog, and cloud), sensors, and the size of the mine structure was one of the threats we had to validate. For this, we proposed a scenario with underground coal mines containing 10 work fronts, something usual in medium and large scale mining in the department of Boyacá, Colombia (region that supports part of the doctoral thesis). The simulated sensors covered the generation of data for the variables required by Colombian mining regulations (seven types of gases, temperature, and wind speed). The applications performed the operations that are also required by the regulation. Finally, we provisioned 68 AWS EC2 instances (63 edge nodes, 3 fog nodes, and 2 cloud nodes).